Geochemistry Geophysics Geosystems G3
AN ELECTRONIC JOURNAL OF THE EARTH SCIENCES
Published by AGU and the Geochemical Society

Article
Volume 4, Number 8
8 August 2003
8712, doi:10.1029/2002GC000406
ISSN: 1525-2027

Oxygen isotope geochemistry of the second HSDP core

Zhengrong Wang, Nami E. Kitchen, and John M. Eiler

Division of Geological and Planetary Sciences, California Institute of Technology, M/C 100-23, Pasadena, California 91125, USA (wzhr@gps.caltech.edu; eiler@gps.caltech.edu)

[1] Oxygen isotope ratios were measured in olivine phenocrysts (~1 mm diameter), olivine microphenocrysts (generally ~100–200 μm diameter), glass, and/or matrix from 89 samples collected from depths down to 3079.7 m in the second, and main, HSDP core (HSDP-2). Olivine phenocrysts from 11 samples from Mauna Loa and 34 samples from the submarine section of Mauna Kea volcano have $\delta^{18}O$ values that are similar to one another (5.11 ± 0.10‰, 1σ, for Mauna Loa; 5.01 ± 0.07‰, for submarine Mauna Kea) and within the range of values typical of olivines from oceanic basalts ($\delta^{18}O$ of ~5.0 to 5.2‰). In contrast, $\delta^{18}O$ values of olivine phenocrysts from 20 samples taken from the subaerial section of Mauna Kea volcano (278 to 1037 mbsl) average 4.79 ± 0.13‰. Microphenocrysts in both the subaerial (n = 2) and submarine (n = 24) sections of Mauna Kea are on average ~0.2‰ lower in $\delta^{18}O$ than phenocrysts within the same stratigraphic interval; those in submarine Mauna Kea lavas have an average $\delta^{18}O$ of 4.83 ± 0.11‰. Microphenocrysts in submarine Mauna Kea lavas and phencrysts in Mauna Loa lavas are the only population of olivines considered in this study that are typically in oxygen isotope exchange equilibrium with coexisting glass or groundmass. These data confirm the previous observation that the stratigraphic boundary between Mauna Loa and Mauna Kea lavas defines a shift from "normal" to unusually low $\delta^{18}O$ values. Significantly, they also document that the distinctive ^{18}O-depleted character of subaerial Mauna Kea lavas is absent in phenocrysts of submarine Mauna Kea lavas. Several lines of evidence suggest that little if any of the observed variations in $\delta^{18}O$ can be attributed to subsolidus alteration or equilibrium fractionations accompanying partial melting or crystallization. Instead, they reflect variable proportions of an ^{18}O-depleted source component or contaminant from the lithosphere and/or volcanic edifice that is absent in or only a trace constituent of subaerial Mauna Loa lavas, a minor component of submarine Mauna Kea lavas, and a major component of subaerial Mauna Kea lavas. Relationships between the $\delta^{18}O$ of phenocrysts, microphenocrysts, and glass or groundmass indicate that this component (when present) was added over the course of crystallization-differentiation. This process must have taken place in the lithosphere and most likely at depths of between ~5 and 15 km. We conclude that the low-$\delta^{18}O$ component is either a contaminant from the volcanic edifice that was sampled in increasingly greater proportions as the volcano drifted off the center of the Hawaiian plume or a partial melt of low-$\delta^{18}O$, hydrothermally altered perdotites in the shallow Pacific lithosphere that increasingly contributed to Mauna Kea lavas near end of the volcano's shield building stage. The first of these alternatives is favored by the difference in $\delta^{18}O$ between subaerial and submarine Mauna Kea lavas, whereas the second is favored by systematic differences in radiogenic and trace element composition between higher and lower $\delta^{18}O$ lavas.

Components: 15,794 words, 11 figures, 2 tables.

Keywords: oxygen isotopes; Mauna Kea; Hawaii; HSDP.

Index Terms: 3640 Mineralogy and Petrology: Igneous petrology; 1040 Geochemistry: Isotopic composition/chemistry; 8499 Volcanology: General or miscellaneous.

Received 15 July 2002; **Revised** 21 May 2003; **Accepted** 2 June 2003; **Published** 8 August 2003.

Wang, Z., N. E. Kitchen, and J. M. Eiler, Oxygen isotope geochemistry of the second HSDP core, *Geochem. Geophys. Geosyst.*, *4*(8), 8712, doi:10.1029/2002GC000406, 2003.

Theme: Hawaii Scientific Drilling Project **Guest Editors:** Don DePaolo, Ed Stolper, and Don Thomas

1. Introduction

[2] Rocks recovered by the second HSDP core (“HSDP-2”) provide the first opportunity to examine a large fraction of the temporal evolution of a single oceanic intraplate volcano. In this paper, we document and discuss the significance of oxygen isotope variations of olivines and coexisting phases in rocks recovered by this core.

[3] At the outset of this study, more was known about the oxygen isotope geochemistry of Hawaiian lavas than of any other basaltic volcanic center, with the possible exception of Iceland [*Kyser et al.*, 1981, 1982; *Garcia et al.*, 1989, 1993, 1998; *Harmon and Hoefs*, 1995; *Eiler et al.*, 1996a, 1996b]. These previous studies showed that many Hawaiian lavas have low $\delta^{18}O$ values ($\equiv[^{18}O/^{16}O/0.0020052 - 1]\cdot 1000$) compared to most terrestrial basalts, and that this characteristic is most strongly expressed in shield-building lavas of the “Kea trend” volcanoes (i.e., Kilauea, Mauna Kea, Kohala and Haleakala). Several hypotheses have been put forward to explain this phenomenon, including (1) ^{18}O depletion of primitive lower-mantle that is presumed to core the Hawaiian plume [*Harmon and Hoefs*, 1995], (2) entrainment of ^{18}O-depleted, recycled oceanic lithosphere within the Hawaiian plume [*Lassiter and Hauri*, 1998], (3) contamination of Hawaiian magmas by ^{18}O-depleted rocks in the current Pacific lithosphere [*Eiler et al.*, 1996b], and (4) contamination of Hawaiian magmas by hydrothermally altered, low-$\delta^{18}O$ rocks in the volcanic edifice (suggested by *Garcia et al.* [1998] for recent Puu Oo lavas; the significance of this process for other Hawaiian lavas has not been explored).

[4] In this study, we analyzed oxygen isotope compositions of olivines and coexisting phases from subaerial Mauna Loa lavas, both subaerial and submarine Mauna Kea lavas, and hyaloclastites and intrusives in the submarine Mauna Kea section. These data confirm the previous observation [*Eiler et al.*, 1996a] that the stratigraphic boundary between Mauna Loa and Mauna Kea marks a shift from “normal” to unusually low $\delta^{18}O$ values, respectively. Additionally, we find that coarse olivine phenocrysts in submarine Mauna Kea lavas and hyaloclastites are “normal” in $\delta^{18}O$ rather than ^{18}O-depleted like subaerial Mauna Kea lavas. Finally, we find there is a systematic difference in $\delta^{18}O$ between coarse phenocrysts and microphenocrysts in the submarine Mauna Kea lavas—the former are similar in $\delta^{18}O$ to other oceanic basalts whereas the latter are distinctly lower in $\delta^{18}O$. We discuss several models for these stratigraphic trends and examine them in light of geochemical and petrologic data presented in other articles in this theme.

2. Sampling and Analytical Techniques

[5] Oxygen isotope ratios were analyzed in olivines, glass and/or groundmass from 89 samples of 88 tholeiites and one alkalic basalt in the HSDP-2 core from depths down to 3079.7 m below sea level (mbsl); these data are presented in Table 1. Our sampling of the submarine Mauna Kea section includes 27 pillow lavas, 21 hyaloclastites, 7 massive and 3 intrusive rocks. We refer to pillow basalts, massive lava flows and hyaloclastites as “lavas” in the remainder of this paper unless we wish to make a particular distinction among these subtypes of basalts. Most samples below 560 mbsl are from splits of the geochemical reference suite also analyzed in the accompanying articles in this theme. Samples from above 560 mbsl were collected by the authors from the portion of the HSDP-2 core stored at Caltech, and were generally taken from within 1.5 m of a reference suite sample; the exception is sample SR0133-0.04, which is 4.4 m below the sample SR0131-6.92

from the geochemical reference suit. All of our samples were taken from within a stratigraphic unit sampled by the geochemical reference suite. Further details for correlating our samples with those in other papers are given in Table 1.

[6] All mineral, glass and groundmass separates were prepared by crushing, sieving, ultrasonicating in distilled water or 1N HCl, ultrasonicating in ethanol, drying, and handpicking under a binocular microscope. Mineral, glass and groundmass fragments containing visible inclusions and alteration products were discarded during handpicking.

[7] Most data are for large ($\geq$1 mm) phenocrysts of olivine. However, we also recovered and analyzed fine-grained (usually $\sim$100 to 200 μm diameter) separates of olivine microphenocrysts from 26 samples. We only separated microphenocrysts from lavas that are poor in coarser phenocrysts in order to avoid the possibility of mistaking small fragments of phenocrysts for microphenocrysts. The separated microphenocrysts are more susceptible to subsolidus alteration and might have formed by a different generation of olivine crystallization from that which formed coarse phenocrysts. Therefore we distinguish between these two groups of olivine analyses in Table 1, all figures and throughout our discussion. Previous studies of the petrography and mineral chemistry of Hawaiian lavas have shown that coarse olivine phenocrysts and/or xenocrysts are relatively magnesian (forsterite contents between $\sim$88 and 86%) and many are strained—suggesting that they formed relatively early in the differentiation history of their host lavas or other magmas in the Hawaiian edifice and spent some time as components of cumulate piles before being brought to the surface [*Clague et al.*, 1995; *Baker et al.*, 1996]. In contrast, microphenocrysts are less magnesian (typical forsterite contents of $\sim$82 to 80%, extending down to $\sim$50% on grain rims) and are inferred to be relatively late-stage precipitates from their host lavas. We checked that differences between these two populations previously identified in thin section correspond to differences between our "phenocryst" versus "microphenocryst" mineral separates by making electron microprobe measurements of splits from two of our samples (Table 2). Our separated phenocrysts from sample SR0762-4.60 have forsterite contents of $\sim$87.3 ± 0.8 mole% whereas our separated microphenocrysts from sample SR0907-1.65 have cores with $\sim$81.6 ± 0.5 mole% forsterite.

[8] Glass separates were recovered from thin rims surrounding olivine phenocrysts in hyaloclastites or from thick glassy rinds of pillow basalts. Analyzed glass fragments were dark brown and semi-transparent; fragments that appeared altered (e.g., opaque and lacking glassy luster) were not analyzed. "matrix" separates consisted of fine-grained aggregates of glass and minerals. Two separates of matrix from sample SR0157-7.17 were analyzed: one having a particle size of 200 to 300 μm ("matrix-a"; consisting of dark gray aggregates of glass and mafic minerals) and one having a size <150 μm ("matrix-b"; consisting of light gray aggregates dominated by plagioclase). The first of these is most like matrix and glass recovered from other samples and is the measurement from this sample plotted and discussed in the following sections.

[9] All mineral, glass and matrix separates were analyzed by laser fluorination at the California Institute of Technology using methods previously described by *Eiler et al.* [2000a, 2000b] and based on methods described by *Sharp* [1990] and *Valley et al.* [1995]. A total of 67 UWG-2 (garnet), 33 SCO2 (olivine), 15 SCO3 (olivine) and 26 ALV526 (glass) standards were analyzed interspersed with analyses of samples. Results for these standards are as follows: UWG-2 = 5.77 ± 0.10‰, SCO2 = 5.25 ± 0.09‰, SCO3 = 5.31 ± 0.08‰ and ALV526 = 5.36 ± 0.09‰ (all standard deviations refer to long-term reproducibility of raw measurements and are 1σ); these values compare with accepted values of: UWG-2 = 5.80‰, SCO2 = 5.25‰, SCO3 = 5.35‰ and ALV526 = 5.40‰ [*Valley et al.*, 1995; *Eiler et al.*, 2000a, 2000b]. All $\delta^{18}O$ values for unknowns measured on a given day were corrected by the difference between measured and accepted values for standards on that day. All measurements of unknown samples were replicated, generally in duplicate but some between three and seven times; standard deviations for each sample are reported in the Table 1. Olivines from a few samples were not replicated to within our

Table 1. Oxygen Isotope Compositions of Materials From the HSDP-2 Core[a]

Sample	Depth,[b] mbsl	Unit[c]	Rock Type[d]	Material	$\delta^{18}O$, ‰	1 σ	Note[e]
SR0008-3.12	9.7	U0002	Mauna Loa subaerial	Olivine	5.13	0.05	W
SR0023-2.90	34.1	U0006	Mauna Loa subaerial	Olivine	5.15	0.02	W
				Matrix	5.36	0.13	W
SR0031-0.52	45.5	U0007	Mauna Loa subaerial	Olivine	5.14	0.05	W
				Glass	5.42	0.08	W
SR0036-2.18	53.7	U0008	Mauna Loa subaerial	Olivine	5.02	0.11	W
SR0066-0.13	98.8	U0018	Mauna Loa subaerial	Olivine	4.93	0.06	W
SR0067-0.33	100.4	U0018	Mauna Loa subaerial	Olivine	5.02	0.05	W
SR0098-0.00	177.1	U0028	Mauna Loa subaerial	Olivine	5.27	0.05	W
SR0100-7.33	185.6	U0029	Mauna Loa subaerial	Olivine	5.14	0.10	W
SR0104-5.46	197.5	U0032	Mauna Loa subaerial	Olivine	5.14	0.04	W
SR0113-6.56	222.4	U0036	Mauna Loa subaerial	Olivine	5.25	0.05	W
SR0118-0.40	234.9	U0037	Mauna Loa subaerial	Olivine	5.05	0.06	W
SR0133-0.04	278.8	U0048	Mauna Kea subaerial	Olivine	4.78	0.07	W
				Glass	4.36	0.10	W
SR0136-6.33	290.0	U0053	Mauna Kea subaerial	Olivine	4.64	0.07	W
				Glass	4.13	0.06	W
SR0137-6.08	293.0	U0053	Mauna Kea subaerial	Olivine	4.60	0.02	W
SR0141-8.83	*306.0*	*U0056*	*Mauna Kea subaerial*	*Olivine*	*4.49*	*0.09*	*W*
				Matrix	4.39	0.02	W
SR0148-8.67	326.7	U0060	Mauna Kea subaerial	Olivine	4.77	0.15	W
SR0157-7.17	353.2	U0061	Mauna Kea subaerial	Olivine	4.60	0.04	W
				Matrix-a	4.74	0.10	W
				Matrix-b	5.11	0.02	W
SR0175-5.21	398.0	U0073	Mauna Kea subaerial	Olivine	4.71	0.10	W
SR0184-4.25	421.5	U0076	Mauna Kea subaerial	Olivine	4.65	0.04	W
SR0193-1.83	444.1	U0080	Mauna Kea subaerial	Olivine	4.66	0.08	W
				Matrix	4.67	0.03	W
SR0206-0.30	469.3	U0084	Mauna Kea subaerial	Olivine	4.97	0.05	W
SR0213-3.58	492.5	U0088	Mauna Kea subaerial	Olivine	4.72	0.15	W
SR0222-3.67	516.6	U0092	Mauna Kea subaerial	Olivine	4.77	0.03	W
SR0233-1.08	542.9	U0094	Mauna Kea subaerial	Olivine	4.71	0.12	W
SR0267-6.85	615.8	U0107	Mauna Kea subaerial	Olivine	4.97	0.09	R
SR0276-7.85	636.0	U0110	Mauna Kea subaerial	Olivine	4.78	0.15	R
SR0328-3.10	759.8	U0127	Mauna Kea subaerial	Olivine	4.71	0.16	R
SR0346-5.60	812.7	U0136	Mauna Kea subaerial	Olivine	4.93	0.13	R
SR0354-7.75	833.9	U0138	Mauna Kea subaerial	Olivine	5.06	0.07	R
SR0372-2.80	871.2	U0142	Mauna Kea subaerial	Olivine	4.62	0.07	R
SR0379-3.00	888.4	U0144	Mauna Kea subaerial	Olivine	4.89	0.09	R
SR0423-3.65	1012.4	U0157	Mauna Kea subaerial	Olivine	4.89	0.06	R
SR0431-8.50	*1037.7*	*U0160*	*Mauna Kea subaerial*	*Olivine*	*4.72*	*0.08*	*R*
SR0455-7.40	1098.2	U0179	massive	Olivine	4.95	0.08	R
SR0512-4.70	1294.4	U0194	hyaloclastite	Olivine	5.15	0.06	S
				Glass	5.06	0.05	S
SR0531-4.40	1352.6	U0198	massive	Olivine	4.95	0.06	R
SR0545-8.35	1394.9	U0198	hyaloclastite	Olivine	4.95	0.02	R
SR0548-8.00	1404.1	U0199	massive	Olivine	5.05	0.08	R
SR0560-7.50	1435.4	U0202	hyaloclastite	Olivine	5.03	0.02	R
SR0582-10.00	1497.7	U0207	massive	Olivine	5.01	0.09	R
				Glass	5.10	0.06	R
SR0594-8.70	1521.4	U0213	massive	Olivine	4.98	0.15	R
SR0596-5.55	1526.3	U0214	hyaloclastite	Olivine	5.01	0.15	S
SR0603-8.90	1548.2	U0216	hyaloclastite	Olivine	4.98	0.07	R
SR0622-7.10	1581.2	U0218	hyaloclastite	Olivine	5.01	0.15	R
SR0655-4.00	1678.7	U0238	hyaloclastite	Olivine	4.99	0.07	R
SR0664-5.10	1705.5	U0238	hyaloclastite	Olivine	5.02	0.08	R
SR0675-6.90	1739.3	U0243	hyaloclastite	Olivine	5.02	0.08	R
SR0683-5.75	1763.2	U0245	massive	Olivine	5.14	0.07	R
SR0686-5.1	*1771.6*	*U0248*	*hyaloclastite*	*Olivine*	*4.78*	*0.05*	*C*
				Glass	5.17	0.05	C

Table 1. (continued)

Sample	Depth,[b] mbsl	Unit[c]	Rock Type[d]	Material	$\delta^{18}O$, ‰	1 σ	Note[e]
SR0696-8.4	*1797.4*	*U0254*	*hyaloclastite*	*Olivine*	*4.99*	*0.10*	*C*
				Glass	5.14	0.11	C
SR0697-8.1	*1800.2*	*U0254*	*hyaloclastite*	*Olivine*	*4.79*	*0.10*	*C*
				Glass	5.30	0.17	C
SR0698-5.6	*1802.5*	*U0255*	*hyaloclastite*	*Olivine*	*4.90*	*0.13*	*C*
				Glass	4.66	0.10	C
SR0699-5.55	*1805.7*	*U0256*	*hyaloclastite*	*Olivine*	*4.83*	*0.05*	*C*
				Glass	5.24	0.05	C
SR0709-13.35	1852.0	U0261	hyaloclastite	Olivine	5.02	0.02	R
SR0714-11.55	1883.6	U0263	intrusive	Olivine	5.08	0.11	R
SR0720-18.25	1921.6	U0268	intrusive	Olivine	4.95	0.08	R
SR0741-7.90	2009.8	U0278	Pillow	Olivine	4.99	0.08	R
SR0750-12.45	2062.7	U0283	Pillow	Olivine	4.97	0.03	R
SR0756-13.2	2098.6	U0284	Pillow	Olivine	5.03	0.08	R
SR0762-4.60	2123.7	U0284	Pillow	Olivine	4.99	0.16	R
SR0768-11.20	*2157.4*	*U0285*	*hyaloclastite*	*Olivine*	*4.72*	*0.05*	*R*
				Glass	5.07	0.05	R
SR0778-3.20	*2218.2*	*U0287*	*hyaloclastite*	*Olivine*	*5.10*	*0.11*	*R*
				Glass	5.13	0.07	R
SR0780-20.80	*2236.7*	*U0288*	*Pillow*	*Olivine*	*4.75*	*0.05*	*R*
				Glass	5.15	0.07	R
SR0792-6.20	*2285.2*	*U0290*	*Pillow*	*Olivine*	*4.84*	*0.05*	*R*
				Glass	5.22	0.05	R
SR0796-6.70	*2300.2*	*U0290*	*Pillow*	*Olivine*	*5.05*	*0.03*	*R*
				Glass	5.39	0.07	R
SR0800-13.20	*2321.6*	*U0291*	*Pillow*	*Olivine*	*4.94*	*0.05*	*R*
SR0807-3.70	*2340.7*	*U0292*	*Pillow*	*Olivine*	*4.88*	*0.08*	*R*
				Glass	5.20	0.05	R
SR0814-14.40	*2357.0*	*U0292*	*Pillow*	*Olivine*	*4.69*	*0.08*	*R*
SR0814-17.60	*2357.4*	*U0292*	*Pillow*	*Olivine*	*4.83*	*0.14*	*W*
SR826-13.8	*2411.4*	*U0293*	*Pillow*	*Olivine*	*4.82*	*0.04*	*W*
SR0826-20.60	*2414.1*	*U0293*	*Pillow*	*Olivine*	*4.71*	*0.08*	*R*
SR829-3.40	*2426.7*	*U0293*	*Pillow*	*Olivine*	*4.76*	*0.14*	*W*
		U0293	*hyaloclastite*	*Olivine*	*4.78*	*0.05*	*W*
SR0836-5.80	*2467.3*	*U0295*	*Pillow*	*Olivine*	*4.81*	*0.05*	*R*
SR0837-4.20	2472.8	U0296	Pillow	Olivine	5.03	0.05	W
		U0296	hyaloclastite	Olivine	5.04	0.05	W
SR0843-8.70	2511.5	U0302	massive	Olivine	4.99	0.05	W
SR0846-2.80	2525.4	U0303	hyaloclastite	Olivine	4.88	0.06	R
SR0860-8.10	2615.0	U0310e	Pillow	Olivine	5.01	0.02	R
SR0871-13.00	*2654.1*	*U0312*	*Pillow*	*Olivine*	*4.87*	*0.02*	*R*
SR0891-15.10	*2730.2*	*U0316*	*Pillow*	*Olivine*	*4.84*	*0.04*	*R*
SR0896-2.40	*2759.3*	*U0319*	*hyaloclastite*	*Olivine*	*4.76*	*0.08*	*R*
SR0899-4.40	2770.9	U0320	Pillow	Olivine	4.84	0.05	R
SR0907-1.65	*2789.9*	*U0321*	*Pillow*	*Olivine*	*4.65*	*0.07*	*R*
SR0913-2.4	2825.8	U0327	Intrusive	Olivine	4.93	0.15	R
SR0916-1.15	2837.6	U0330	Pillow	Olivine	5.04	0.05	R
				Matrix	5.06	0.09	R
SR0930-15.85	2919.5	U0333	Pillow	Olivine	5.14	0.02	R
SR0939-18.10	2961.0	U0335a	Pillow	Olivine	5.08	0.02	R
SR0954-8.00	3009.2	U0339	Pillow	Olivine	4.98	0.04	R
SR0964-4.30	3058.0	U0340e	Pillow	Olivine	5.02	0.13	R
SR0967-2.75	*3068.9*	*U0343a*	*Pillow*	*Olivine*	*4.94*	*0.08*	*R*

[a] Italicized entries are data for olivine microphenocrysts. All other olivine analyses are for coarse (1 mm and larger) olivine phenocrysts.
[b] Depth is in meters below sea level (mbsl).
[c] Units defined by the HSDP-2 stratigraphic column.
[d] Petrological description from the HSDP-2 core log.
[e] W, sampled by authors; R, from the HSDP-2 reference suite; C, sampled by Caroline Seaman; S, sampled by Sujoy Mukhopadhyay.

Table 2. Magnesium Numbers of Representative Grains From Olivine Separates

	Average
Coarse Phenocrysts; Sample SR0762-4.60	
88.6; 86.6; 87.6; 87.6; 87.9; 88.4; 88.6; 87.9; 87.1; 87.5; 86.9; 87.0; 86.0	87.3 ± 0.8
Microphenocrysts; Sample SR0907-1.65	
82.0; 81.3; 81.1; 82.2; 80.8; 81.9; 82.0	81.6 ± 0.5

nominal analytical precision, suggesting that they are isotopically heterogeneous. These samples do not appear to be outliers to any of the stratigraphic or geochemical trends discussed below. We analyzed olivines from two to four different samples in each of nine stratigraphic units (units U0018, U0053, U0238, U0254, U0284, U0290, U0292, U0293, and U0296); average values for of $\delta^{18}O_{olivine}$ for the related samples are usually within analytical uncertainty of one another, suggesting at least these individual units are isotopically homogeneous. The $\delta^{18}O_{olivine}$ values of pillow basalt are indistinguishable from those of immediately adjacent hyaloclastites in units U0293 and U0296.

3. Results

3.1. Oxygen Isotope Stratigraphy of the HSDP-2 Core

[10] Olivines from the HSDP-2 core have $\delta^{18}O$ values of between 4.49 and 5.27‰ (averaged for each sample; Table 1 and Figure 1a; minima and maxima for individual measurements, before aver-

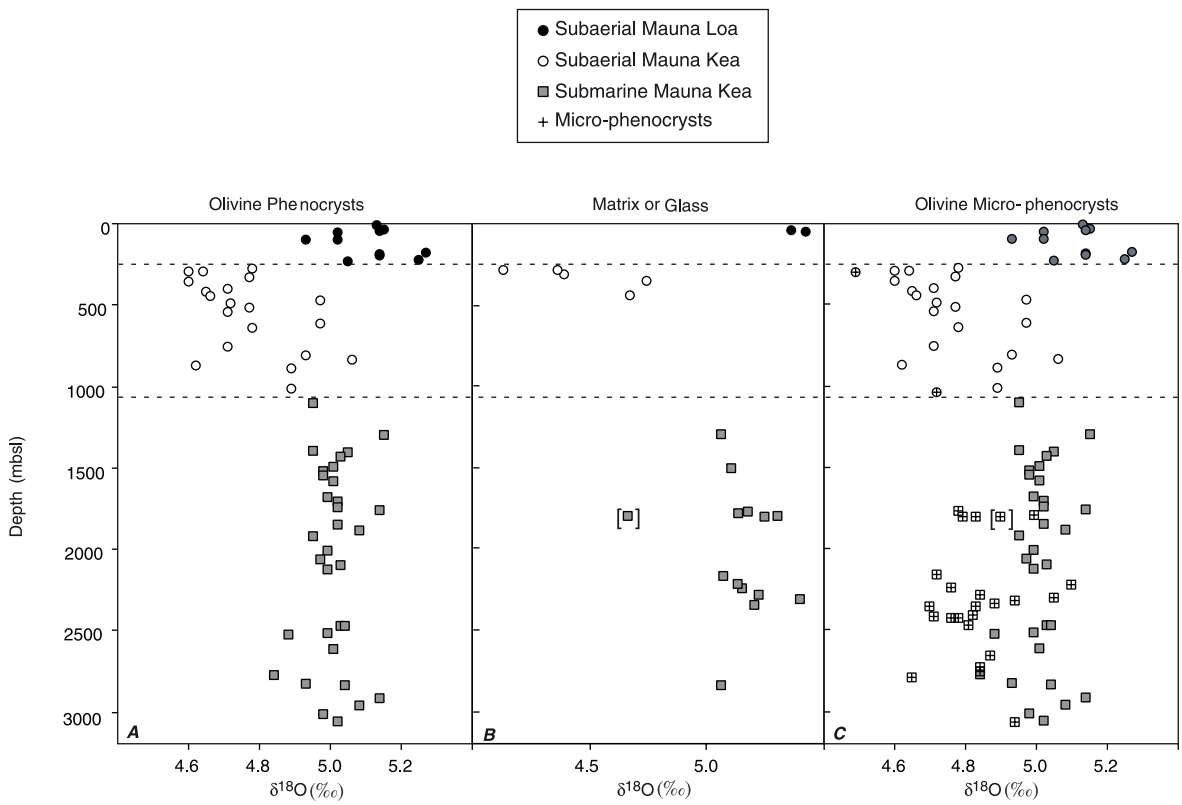

Figure 1. Stratigraphic profiles of the oxygen isotope compositions of materials from the HSDP-2 core, including (A) olivine phenocrysts; (B) glass and nominally fresh volcanic groundmass; and (C) microphenocrysts (data for olivine phenocrysts are reproduced from panel A as faint gray symbols). See legend for symbols used in this and following figures.

aging by hand sample, are 4.36 and 5.43‰). These ranges are similar to those observed in the ~1-km HSDP pilot core (e.g., 4.64 to 5.39‰ when averaged for each sample; *Eiler et al.*, 1996a) and are within the range of values typical of all Hawaiian lavas other than shield-building Koolau and Lanai tholeiites (which are higher in $\delta^{18}O$ [*Eiler et al.*, 1996b]).

[11] Olivine phenocrysts (i.e., as distinct from microphenocrysts) from eleven samples of subaerial Mauna Loa lavas (between 0 and 246 mbsl) and 34 samples of submarine Mauna Kea lavas (greater than 1061 mbsl) have $\delta^{18}O$ values that are similar to one another (5.11 ± 0.10‰, 1σ, versus 5.01 ± 0.07‰, 1σ, respectively) and typical of olivines from other oceanic basalts [*Eiler et al.*, 1997, 2000a, 2000b]. In contrast, olivine phenocrysts from 20 samples of subaerial Mauna Kea lavas (between 246 to 1061 mbsl) have $\delta^{18}O$ values averaging 4.79 ± 0.13‰, 1σ, a lower extreme of 4.60‰, and include many samples having $\delta^{18}O$ values below the lower limits defined by phenocrysts from other sections of the core. Olivine phenocrysts from one sample of alkali basalt from the uppermost portion of the Mauna Kea section of the core (SR133-0.04) have a $\delta^{18}O$ value of 4.78 ± 0.07‰—indistinguishable from tholeiitic lavas in the same section of the core. There is no obvious difference in $\delta^{18}O$ of olivine phenocrysts between hyaloclastites and pillows in a given interval of the core (Table 1). None of the intrusives or massive units have low $\delta^{18}O$ olivine phenocrysts (Table 1).

[12] The stratigraphy of $\delta^{18}O$ values for matrix and glass (Figure 1b) resembles that described above for olivine phenocrysts: the $\delta^{18}O$ values of Mauna Loa lavas and submarine Mauna Kea lavas are relatively high and, with one exception, constant, whereas those for subaerial Mauna Kea lavas are relatively low. However, there are several significant features unique to data for matrix and glass: (1) the range of $\delta^{18}O$ values for matrix and glass is greater—by approximately 50%, relative—than that for olivine phenocrysts; (2) the average values for matrix and glass in Mauna Loa (5.39‰) and submarine Mauna Kea samples (5.13‰) are higher than the averages for coexisting or stratigraphically adjacent olivine phenocrysts — in the direction of the equilibrium melt-olivine fractionation — whereas the average value for matrix and glass in subaerial Mauna Kea samples (4.46‰) is less than that of related olivine phenocrysts — opposite the direction of the equilibrium fractionation; (3) $\delta^{18}O$ values for matrix and glass in submarine Mauna Kea lavas overlap but often fall below the range typical of mid ocean ridge basalt glasses (~5.3 to 5.8‰ [*Eiler et al.*, 2000b; *Eiler*, 2001; K. Cooper, J. M. Eiler, N. Kitchen, P. Asimow, and C. Langmuir, Oxygen isotope evidence for the origin of enriched mantle beneath the Mid-Atlantic Ridge, submitted to *Earth and Planetary Science Letters*, 2003]), whereas olivine phenocrysts in this interval are generally within the range typical of olivine in oceanic basalts; and (4) there is one notable outlier to the otherwise tightly grouped population of glasses in the submarine Mauna Kea section (sample SR697-8.1 from 1802.5 mbsl). This sample contains olivine microphenocrysts that are isotopically similar to those in other submarine Mauna Kea lavas and is not unusual in other aspects of its geochemistry (E. Stolper et al., Glass in the submarine section of the HSDP-2 drill core, Hilo, Hawaii, submitted to *Geochemistry, Geophysics, Geosystems*, 2003) (hereinafter referred to as Stolper et al., submitted manuscript, 2003). We distinguish this unusual sample on all plots where it appears by placing brackets around its symbol.

[13] The stratigraphy of $\delta^{18}O$ values for olivine microphenocrysts (Figure 1c) resembles that described above for olivine phenocrysts (Figure 1a) and matrix or glass (Figure 1b) in that the two subaerial Mauna Kea samples (4.49 and 4.72‰) are lower in $\delta^{18}O$ than the average value for submarine Mauna Kea samples (4.85‰). However, the most noticeable feature of the data for microphenocrysts is that they are consistently lower in $\delta^{18}O$ than phenocrysts in stratigraphically adjacent lavas. In particular, throughout the submarine section of Mauna Kea, all olivine phenocrysts are within or closely approach the lower end of the range typical of oceanic basalts (~5.0 to 5.2‰) whereas microphenocrysts are generally below that range. Histograms illustrating the contrast in $\delta^{18}O$ between phenocrysts and microphenocrysts in the submarine section of Mauna Kea are provided in Figure 2.

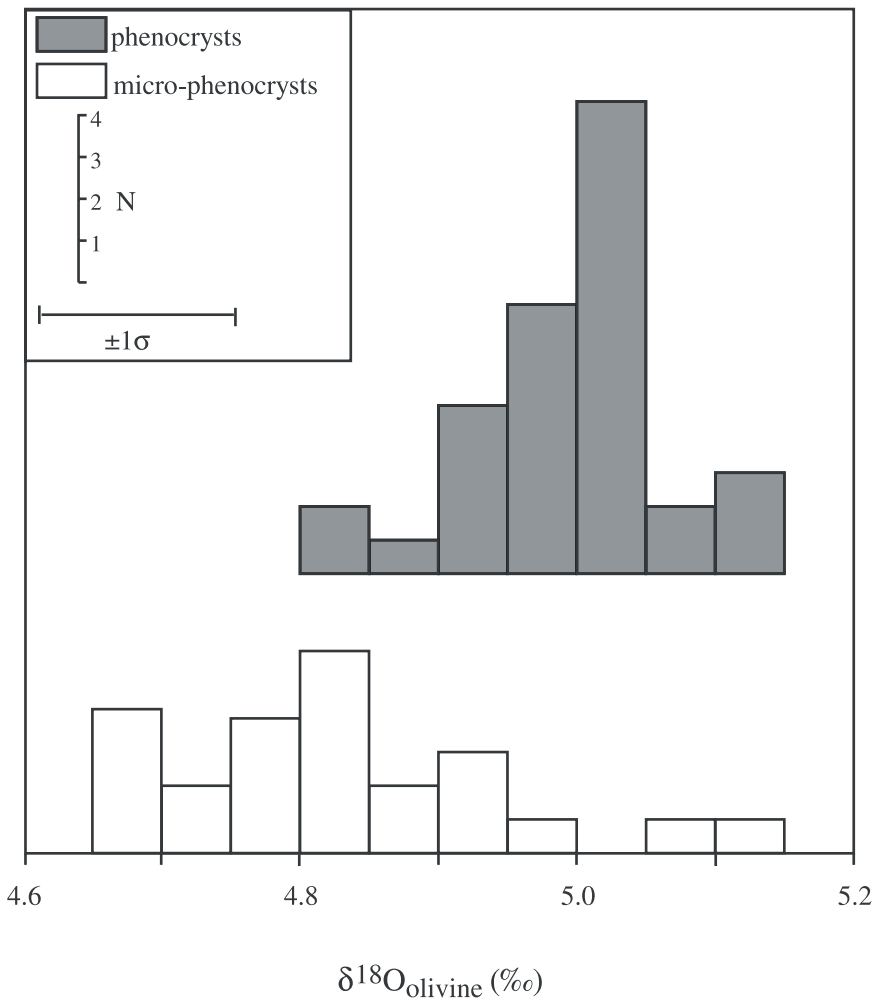

Figure 2. Histograms illustrating the distribution of $d^{18}O$ values for coarse olivine phenocrysts and olivine microphenocrysts in submarine Mauna Kea lavas. Note that microphenocrysts are, on average, ~0.2‰ lower in $\delta^{18}O$ than phenocrysts.

[14] We further examine the relationship between $\delta^{18}O$ values of olivines and host glass or matrix in Figure 3. This plot contains a thick gray line of slope 1 corresponding to a fractionation of 0.4‰ between matrix or glass on one hand and olivine on the other. This is our best estimate of the high-temperature equilibrium fractionation between basaltic melt and olivine based on previous studies of basaltic lavas and experimental studies of oxygen isotope partitioning among melts, glasses, minerals and vapors [*Anderson et al.*, 1971; *Muehlenbachs and Kushiro*, 1974; *Muehlenbachs and Byerly*, 1982; *Matthews et al.*, 1998; *Eiler*, 2001; *Appora et al.*, 2002]. All lavas in which olivine and melt are in high-temperature isotopic equilibrium should plot on or near this line and those that do not have been disturbed by change in $\delta^{18}O$ of olivine, melt, glass and/or matrix groundmass after olivine crystallization. Of phenocryst—glass/matrix pairs, only the two Mauna Loa samples closely approach the equilibrium fractionation and all Mauna Kea samples have fractionations that are significantly too low or even reversed (i.e., opposite in sign to equilibrium value). In contrast, eight of twelve microphenocryst—glass/matrix pairs are indistinguishable from the equilibrium fractionation.

3.2. Comparison of Oxygen Isotope Compositions With Other Geochemical Variables

[15] Figure 4 reproduces values of ε_{Hf} (4a), $^3He/^4He$ (4b), $^{208}Pb^*/^{206}Pb^*$ (4c), and Sm/Yb

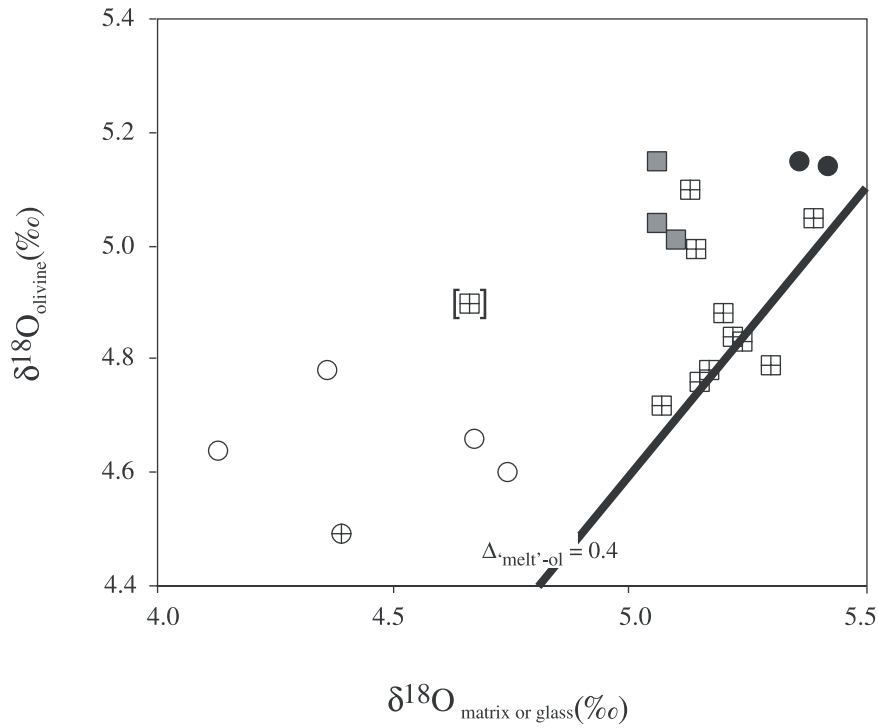

Figure 3. Comparison of $\delta^{18}O$ values measured for olivine phenocrysts or microphenocrysts (vertical axis) to those measured for host glass or groundmass (horizontal axis). Symbols are as in Figure 1. The diagonal gray line is the inferred equilibrium olivine-melt fractionation for basalt at magmatic temperatures; see *Eiler* [2001] for data and references on which this estimate is based. Most microphenocryst—host pairs are in high-temperature isotopic equilibrium, whereas phenocryst—host pairs generally have inferred melt-olivine fractionations that are too small or reversed. The maximum departure from equilibrium (i.e., greatest distance from the gray line) is larger for low-$\delta^{18}O$ samples than for higher $\delta^{18}O$ samples. Disequilibrium fractionations observed in many samples in this study are similar to those previously observed for unaltered Puu Oo lavas [*Garcia et al.*, 1998].

(4d) from the HSDP-2 core (data are taken from *Blichert-Toft et al.* [2003], M. D. Kurz (Helium isotope stratigraphy of the second HSDP core, submitted to *Geochemistry, Geophysics, Geosystems*, 2003) (hereinafter referred to as Kurz, submitted manuscript, 2003), *Eisele et al.* [2003], *Huang and Frey* [2003], and *Feigenson et al.* [2003]). The index $^{208}Pb^*/^{206}Pb^*$ is calculated following *Galer and O'Nions* [1985]. We combined Pb isotope data from *Blichert-Toft et al.* [2003] and *Eisele et al.* [2003] to construct Figure 4c; *Blichert-Toft et al.* [2003] document that these two data sets yield closely similar values of $^{208}Pb^*/^{206}Pb^*$ for the same samples. In addition, Figure 5 reproduces the distributions of SiO_2 contents for submarine Mauna Kea glasses or inferred for subaerial Mauna Kea whole rocks, after normalization for olivine accumulation. These data are taken from Stolper et al. (submitted manuscript, 2003).

[16] There are several similarities and differences between the stratigraphy of $\delta^{18}O$ values (Figure 1) and that of other geochemical variables plotted in Figures 4 and 5:

[17] 1. The boundary between Mauna Loa and Mauna Kea lavas, at which we observe a sharp change from "normal" to unusually low $\delta^{18}O$ values for all analyzed materials, is also a change from less to more radiogenic Hf and He isotope ratios, and from lower to higher $^{208}Pb^*/^{206}Pb^*$ values and Sm/Yb ratios. These differences are the same as those previously observed at the same stratigraphic boundary in the HSDP pilot hole [*Eiler et al.*, 1996a; *Lassiter et al.*, 1996; *Hofmann and Jochum*, 1996] and are consistent with the contrast in oxygen isotopes and other geochemical indices between Mauna Loa and Mauna Kea shield-building lavas exposed at the surface [*Eiler*

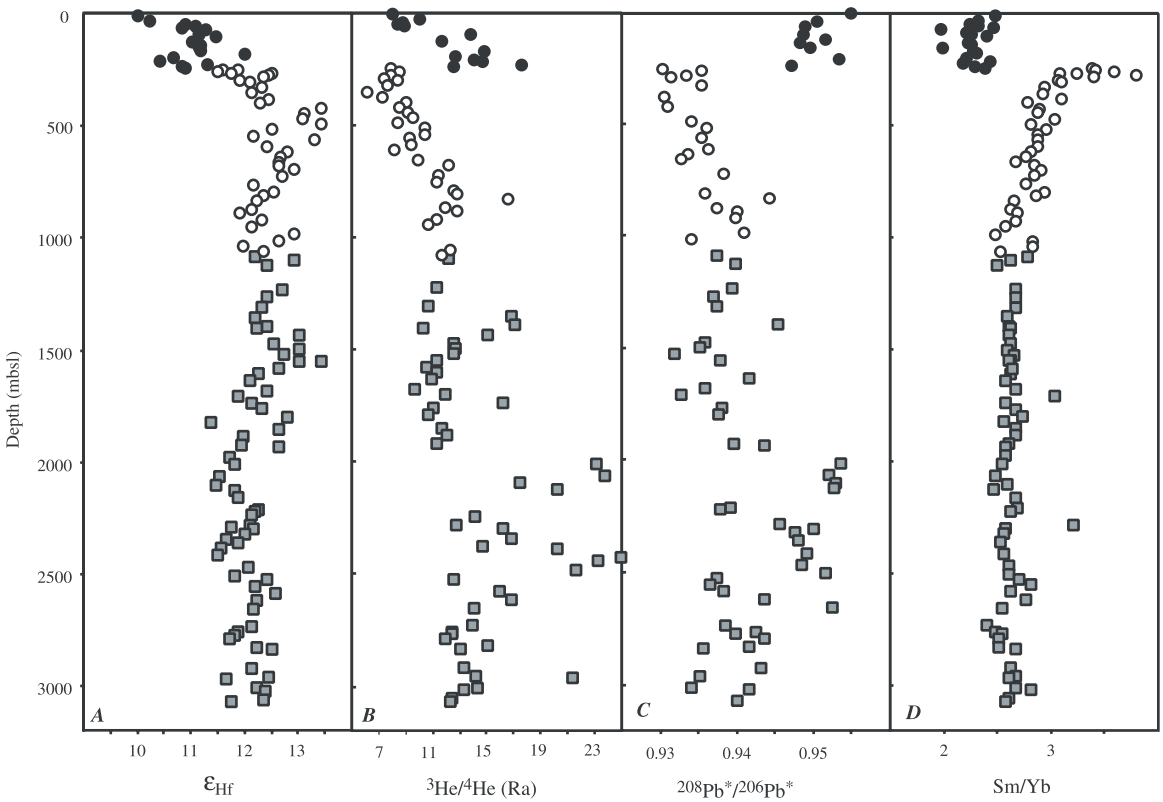

Figure 4. Stratigraphic variations in ε_{Hf} [*Blichert-Toft et al.*, 2003], $^{3}He/^{4}He$ (Kurz, submitted manuscript, 2003), $^{208}Pb^{*}/^{206}Pb^{*}$ (based on data from *Blichert-Toft et al.* [2003] and *Eisele et al.* [2003]), and Sm/Yb [*Feigenson et al.*, 2003] in the HSDP-2 core. See text and Figure 1 for comparisons with the oxygen isotope stratigraphy.

et al., 1996b, and references therein]. Fractionation-normalized SiO_2 contents (Figure 5) were not estimated for Mauna Loa lavas in the HSDP-2 core (Stolper et al., submitted manuscript, 2003). However, previous work suggests this boundary likely marks a significant decrease in silica going down-core from Mauna Loa to Mauna Kea [e.g., *Hauri*, 1996].

[18] 2. The boundary between subaerial and submarine Mauna Kea lavas marks a change in the average oxygen isotope composition of olivine phenocrysts, microphenocrysts, matrix and glass (Figure 1). This change is particularly clear for the olivine phenocryst data, which are the largest and most densely spaced subset of our measurements (Figure 1a). $^{3}He/^{4}He$, Sm/Yb ratios and $^{208}Pb^{*}/^{206}Pb^{*}$ values of subaerial Mauna Kea lavas are also different, on average, than those of submarine Mauna Kea lavas (Figure 4), and thus variations in O, He and Pb isotopes and rare earth element ratios might be caused by similar processes. However, the changes in He and Pb isotopes and Sm/Yb ratios across the subaerial/submarine transition and through the subaerial section are relatively smooth, perhaps caused by a gradual temporal trend, whereas the change in $\delta^{18}O$ of olivine phenocrysts appears relatively sharp. Therefore it also seems possible that these stratigraphic trends have different causes and are only fortuitously correlated with one another.

[19] 3. The distribution of fractionation-corrected SiO_2 contents changes sharply across the subaerial/submarine transition (Stolper et al., submitted manuscript, 2003) (see also Figure 5). In particular, submarine Mauna Kea lavas are characterized by two distinct populations of SiO_2 contents, referred to by Stolper et al. (submitted manuscript, 2003) as the high-SiO_2 and low-SiO_2 series. Neither of these populations contains anomalously low $\delta^{18}O$ olivine phenocrysts (the $\delta^{18}O$ values of glass and microphenocrysts are also similar in both). Intermediate SiO_2 contents are rare in the submarine section of

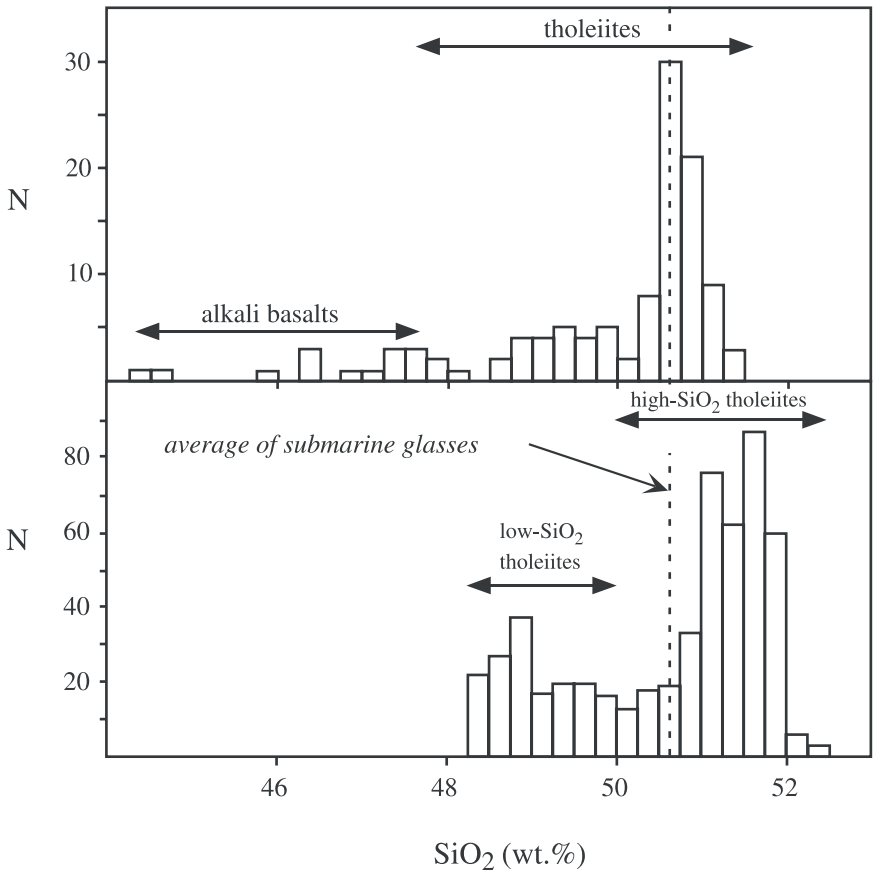

Figure 5. Histograms illustrating the distribution in fractionation-normalized SiO_2 contents of submarine Mauna Kea glasses (lower columns) and subaerial basalts (upper columns). Data from Stolper et al. (submitted manuscript, 2003). Note that submarine lavas are characterized by a bimodal population of higher and lower-SiO_2 lavas. In contrast, subaerial lavas have a unimodal distribution with an average equal to the mean of all submarine lavas.

the core and are always associated with extensive degassing, leading Stolper et al. to suggest they could be mixtures of high-SiO_2 and low-SiO_2 magmas that only encounter one another in a shallow magma reservoir. In contrast, subaerial Mauna Kea tholeites have a unimodal distribution of intermediate SiO_2 contents (i.e., between the low-SiO_2 and high-SiO_2 submarine populations), with a long tail of low-SiO_2 compositions extending toward alkaline post-shield lavas. We find it striking that the transition from bimodal to unimodal SiO_2 contents occurs at the submarine/subaerial transition, and thus coincides with the transition from normal to anomalously low-$\delta^{18}O$ olivine phenocrysts.

[20] 4. There are two intervals of exceptionally high $^3He/^4He$ ratios and $^{208}Pb^*/^{206}Pb^*$ values between 1950 and 2500 mbsl (Figures 4b and 4c). These intervals are discussed at length in several articles in this theme [*Blichert-Toft et al.*, 2003; Kurz, submitted manuscript, 2003; *Eisele et al.*, 2003]. There is no obvious anomaly in the $\delta^{18}O$ of any one analyzed material (phenocryst, microphenocryst, glass or matrix) within the narrow stratigraphic intervals having anomalous He and Pb isotope ratios.

[21] 5. Two intervals of the submarine section of the core are anomalous in their major element chemistry: (1) glasses between 1765 and 1810 mbsl are anomalously rich in K_2O; and (2) glasses between 2235 and 2280 mbsl are unusual in several respects consistent with them being products of unusually low degrees of mantle melting (Stolper et al., submitted manuscript, 2003). There is no obvious relationship between $\delta^{18}O$ of glass or microphenocrysts and K_2O over this first interval, although it is

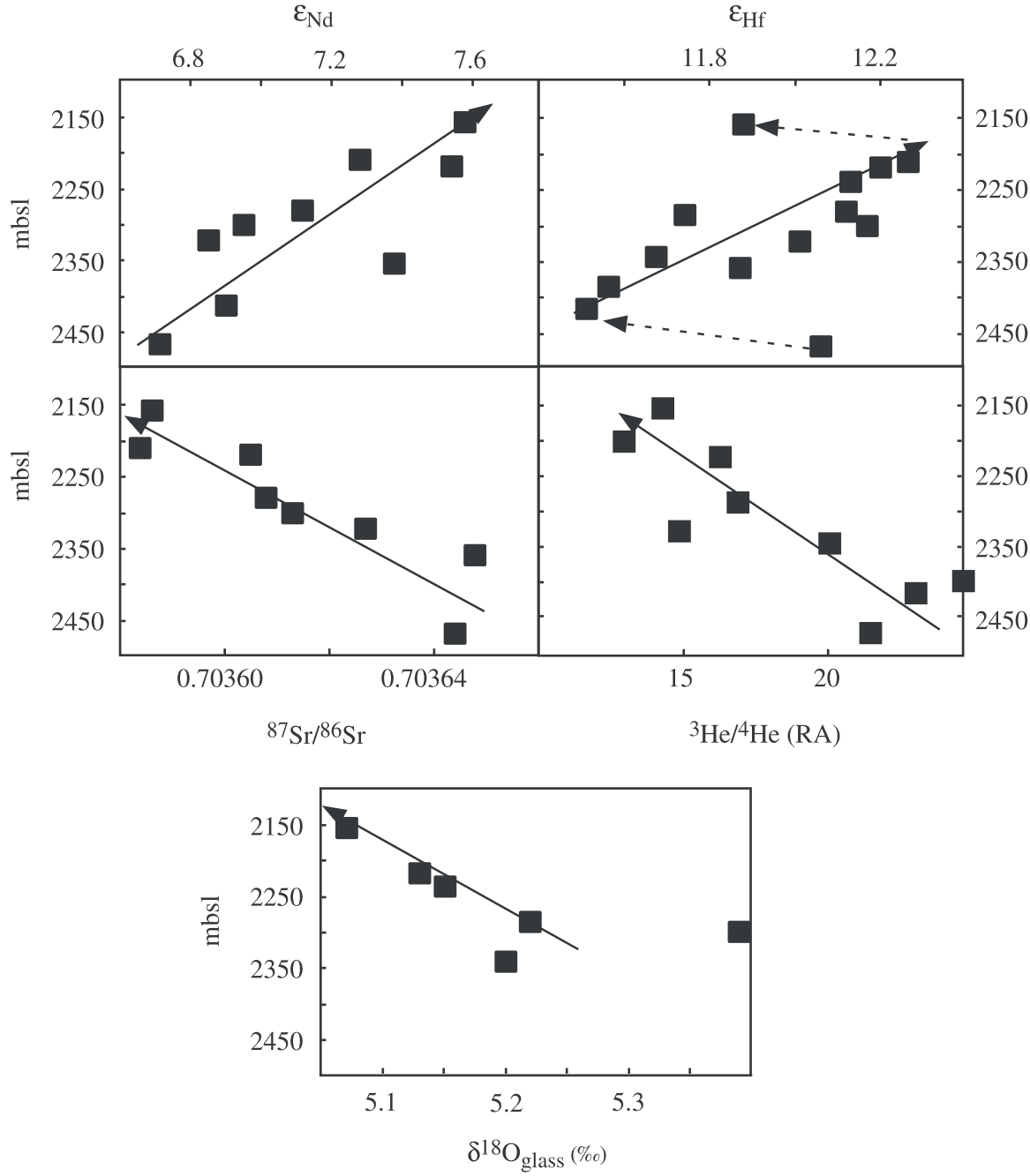

Figure 6. Stratigraphic variations in e_{Nd} (J. G. Bryce and D. J. DePaolo, Sr and Nd isotope stratigraphy of the second HSDP core, submitted to *Geochemistry Geophysics Geosystems*, 2003), e_{Hf}, $^{87}Sr/^{86}Sr$, $^{3}He/^{4}He$ and $\delta^{18}O_{glass}$ over an interval in the submarine Mauna Kea section that is characterized by unusually coherent, monotonic trends in radiogenic isotope composition, perhaps due to unusually simple mixing relationships between isotopically distinct sources. The $\delta^{18}O$ value of glass over this interval decreases monotonically with decreasing depth, suggesting all stratigraphic trends reflect increasing contributions from a component that is relatively low in $\delta^{18}O$, $^{87}Sr/^{86}Sr$ and $^{3}He/^{4}He$ and relatively high in ε_{Nd} and ε_{Hf}. Such simple stratigraphic trends are not seen elsewhere in the Mauna Kea section of the core, either because they are obscured elsewhere by more complex mixing relationships (e.g., involving three or more end-members [*Eisele et al.*, 2003]), or because they are fortuitous here and do not reflect real coupling of these isotopic systems.

noteworthy that it includes sample SR0698-5.6, which has exceptionally low $\delta^{18}O$ glass and an exceptionally low glass-olivine fractionation (Figures 1b and 3). Only one of our samples (SR0780-20.80) is from within the second interval, but we note there is a systematic stratigraphic trend in several radiogenic isotope ratios over the larger, overlapping interval of ~2150 to 2500 mbsl (Figure 6). Six samples from this larger interval were analyzed for oxygen isotope composition of glass, and appear to decrease in $\delta^{18}O$ with decreasing depth, correlated with increases in ε_{Nd} and ε_{HF} and decreases in $^{3}He/^{4}He$ and $^{87}Sr/^{86}Sr$ with decreasing depth (Figure 6; note the stratigraphic trend in ε_{HF} appears more complex at the top and bottom of this interval than do those of other radiogenic isotope ratios). While these trends might reflect coupled, gradual changes over time, note that this interval contains discontinuities in the stratigraphy of SiO_2 and a layer of fine-grained sand that might mark a significant change in deposition rate (Stolper et al., submitted manuscript, 2003).

[22] We further examine relationships between oxygen isotopes and other geochemical variables by plotting $\delta^{18}O$ versus various major-element, trace element and radiogenic isotope indices measured on whole rock splits and glasses from the same samples or nearby samples from the same units (Figures 7a–7e). Figures 7a–7d show that variations in $\delta^{18}O$ of olivine phenocrysts (filled and unfilled circles and squares) are loosely but consistently correlated with other geochemical variables, and that these correlations are defined both by differences between Mauna Loa and Mauna Kea lavas and by variations among Mauna Kea lavas alone. In Figures 7a–7c, these correlations consist of three overlapping but distinguishable groups—(1) Mauna Loa, (2) submarine Mauna Kea, and (3) subaerial Mauna Kea—that differ from one another in average values of $\delta^{18}O$ of olivine phenocrysts and in the other plotted variable. The sense of these trends is that decreasing $\delta^{18}O$ is associated with decreasing Al_2O_3/TiO_2, increasing Sm/Yb, and decreasing V/Ti (the significance of which is discussed below). Figure 7d has a somewhat different appearance: Mauna Loa lavas and submarine Mauna Kea lavas span a large range of generally high $^{3}He/^{4}He$ ratios with "normal" values of $\delta^{18}O$ for olivine phenocrysts, whereas subaerial Mauna Kea lavas define a distinct group that is anomalously low in both $\delta^{18}O$ and $^{3}He/^{4}He$. This figure has the same topology as a plot of $\delta^{18}O_{olivine}$ versus $^{3}He/^{4}He$ for all Hawaiian shield-building lavas [*Eiler et al.*, 1996b]. Data for olivine microphenocrysts generally conform to the trends defined by olivine phenocrysts in Figures 7a–7d; however, four submarine Mauna Kea lavas are exceptions having olivine microphenocrysts with $\delta^{18}O$ values ~0.2‰ lower than olivine phenocrysts in chemically similar (and stratigraphically close) lavas.

[23] Figure 7e compares the $\delta^{18}O$ values of submarine Mauna Kea glasses to MgO contents of glasses from the same units measured by electron microprobe (Stolper et al., submitted manuscript, 2003). For comparison, we also show data for recent lavas from the Puu Oo vents on Kilauea's east rift zone [*Garcia et al.*, 1998]. Excepting the anomalous sample SR0698-5.6 (indicated by brackets), the total range in $\delta^{18}O$ for Mauna Kea glasses (0.32‰) is a small multiple of analytical precision (0.07‰). Nevertheless, they define a positive correlation with MgO (i.e., decreasing MgO is associated with decreasing $\delta^{18}O$). A stronger positive correlation is defined by the more compositionally diverse Puu Oo lavas. This trend is offset toward lower $\delta^{18}O$ values at any given MgO content when compared to submarine Mauna Kea glasses, but is otherwise similar. The anomalous submarine Mauna Kea glass from sample SR0698-5.6 falls on the trend defined by Puu Oo glasses. Finally, we cannot plot matrix samples from subaerial Mauna Kea lavas on Figure 7e because there is no simple way to estimate their MgO contents excluding accumulated olivine. However, these samples appear to have undergone similar extents of differentiation as submarine lavas (Stolper et al., submitted manuscript, 2003) and are consistently ~0.5‰ lower in $\delta^{18}O$ than submarine glasses; thus they likely also fall near the trend defined by Puu Oo glasses.

[24] Trends in Figure 7e indicate that decreasing $\delta^{18}O$ values (from nominally normal toward anomalously low) are associated with increasing degrees of crystallization-differentiation. This result is im-

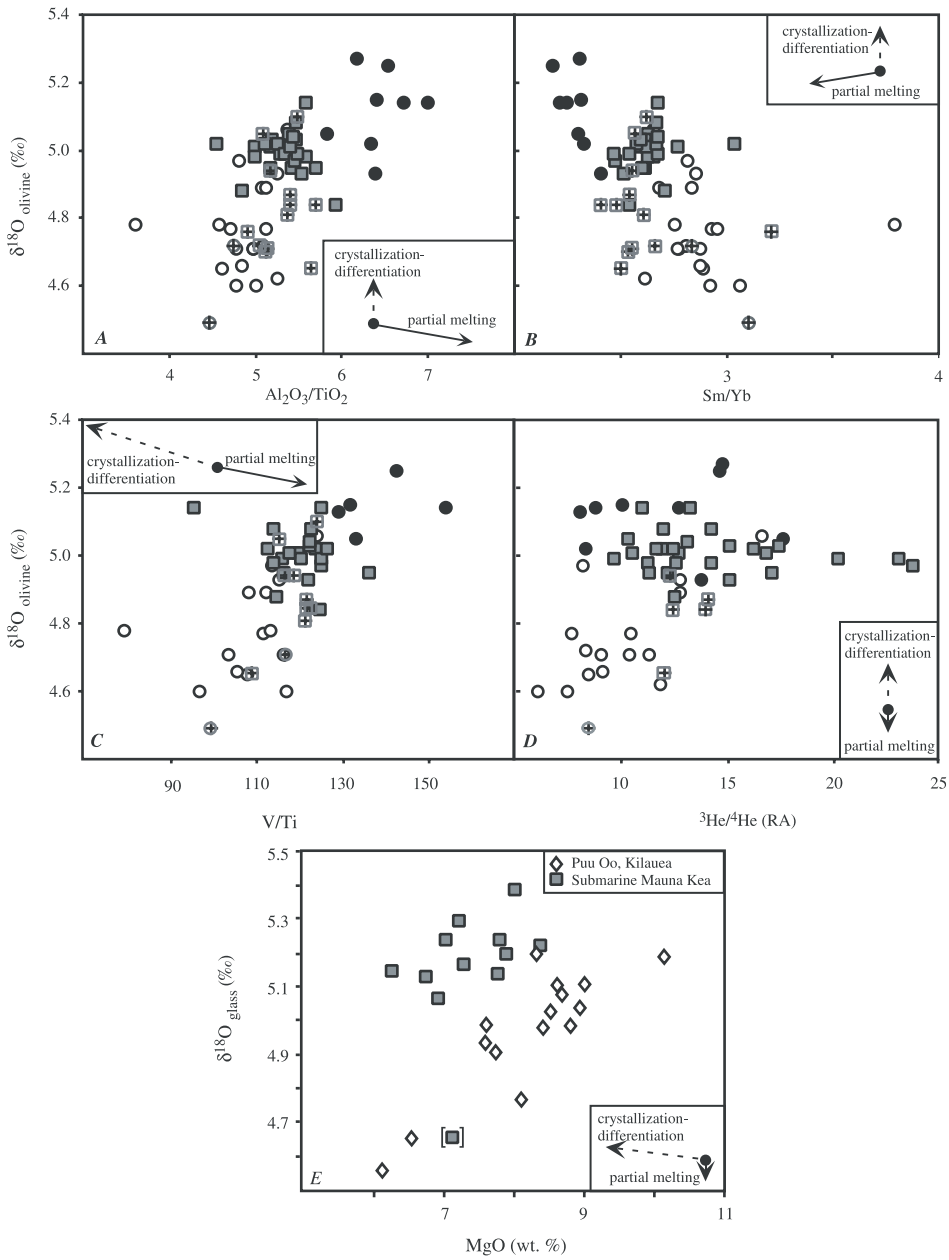

Figure 7. Comparison of $\delta^{18}O$ values for phenocrysts and microphenocrysts from the HSDP-2 core with elemental abundances and radiogenic isotope compositions of host lavas. Panels A through D are plotted using symbols given in Figure 1. Panel E also uses these symbols for submarine Mauna Kea lavas, and shows data for recent lavas from Puu Oo (Kilauea; taken from *Garcia et al.* [1998]) as open diamonds.

portant for the interpretation of our data because it suggests that the dominant process controlling variations in $\delta^{18}O$ is caused by, or at least correlated with, magmatic differentiation rather than partial melting and/or variations among mantle sources. It is difficult to determine whether the same trend exists for the larger data set of olivine phenocrysts and microphenocrysts because the Mg# of each analyzed grain is not known. However, recall that magnesian, coarse olivines presumably crystallized from higher-MgO liquids than did more iron-rich microphenocrysts; thus the difference in $\delta^{18}O$ between these two populations (Figure 2) is consistent with the trends in Figure 7e. Finally, the V/Ti ratio should decrease in residual magma during precipitation of olivine ± chromian

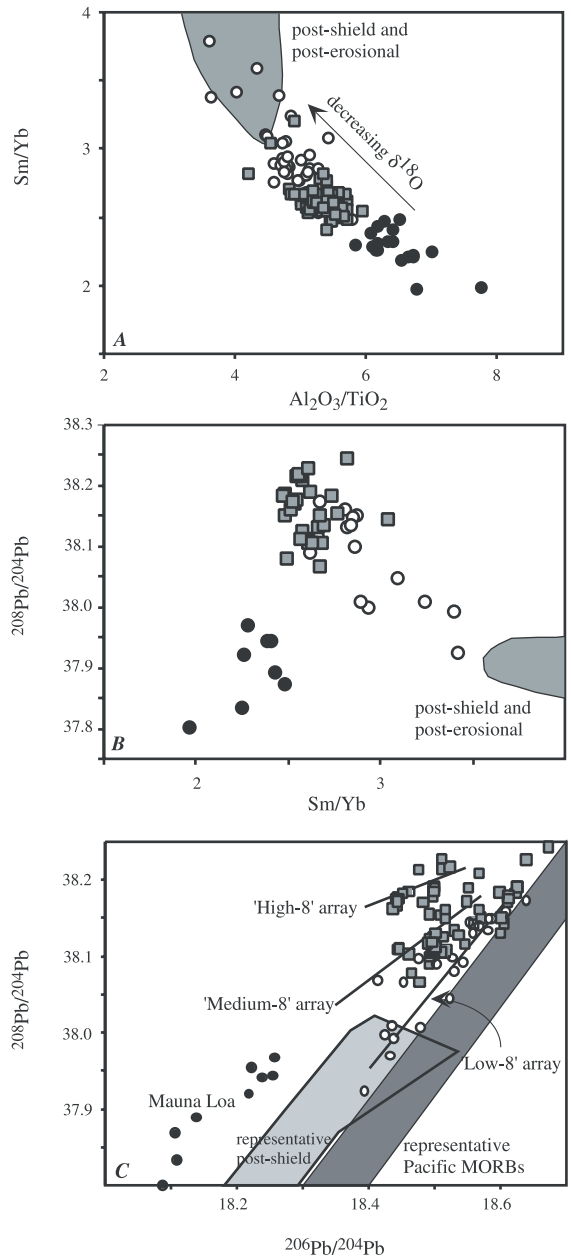

Figure 8. Comparison of Sm/Yb ratios with Al_2O_3/TiO_2 (panel A) and $^{208}Pb/^{204}Pb$ (panel B) in HSDP-2 lavas (data from *Feigenson et al.* [2003], M. Rhodes (Major and minor element concentrations of HSDP2 lavas, submitted to *Geochemistry, Geophysics, Geosystems*, 2003), and *Blichert-Toft et al.* [2003]). In both cases, subaerial Mauna Kea lavas (the lowest-$\delta^{18}O$ subset of the HSDP-2 core) are offset toward the field of compositions defined by post-shield and post-erosional Hawaiian basalts (gray fields; data from *Chen and Frey* [1983], *Hegner et al.* [1986], *West and Leeman* [1987], *Kennedy et al.* [1991], and *Lassiter et al.* [2000], and references therein).

spinel [*Green*, 1994], and neither element is sufficiently compatible for small amounts of accumulated olivine to overwhelm this signal. Therefore the positive trend in Figure 7c is consistent, at least in direction, with trends in Figure 7e.

[25] Finally, we further illustrate geochemical differences between relatively high- and relatively low-$\delta^{18}O$ lavas using plots of Sm/Yb, Al_2O_3/TiO_2 and Pb isotope composition versus one another (Figure 8), on which arrows indicate the direction of decreasing average $\delta^{18}O$ between these groups (based on Figures 1 and 7) and plotted fields permit comparison of these trends with compositions of Pacific MORBs and/or post-shield and post-erosional Hawaiian lavas [*Hegner et al.*, 1986; *West and Leeman*, 1987; *White et al.*, 1987; *Kennedy et al.*, 1991; *Schiano et al.*, 1997; *Lassiter et al.*, 2000]. Figures 8a and 8b show that the transition from higher to lower $\delta^{18}O$ values is associated with a shift in major-element, minor-element and radiogenic isotope composition toward those of post-shield and post-erosional basalts, which have been suggested to sample a source related to local asthenospheric and/or lithospheric mantle [e.g., *Chen and Frey*, 1983; see also *Huang and Frey*, 2003; *Feigenson et al.*, 2003]. It is counterintuitive that this component should be characterized by high Sm/Yb because the oceanic asthenosphere and lithospheric mantle are lower in this ratio than putative plume sources (see discussion by *Lassiter and Hauri* [1998]). This can be explained if the high Sm/Yb, isotopically MORB-like component is a low-degree lithospheric and/or asthenospheric melt, such that its abundance ratios of moderately incompatible elements are fractionated with respect to their sources [*Chen and Frey*, 1983].

[26] *Eisele et al.* [2003] organize Pb isotope variations in HSDP-2 lavas into three groups—"High-8", "Middle-8", and "Low-8"—each of which defines a linear trend in a plot of $^{208}Pb/^{204}Pb$ versus $^{206}Pb/^{204}Pb$ (Figure 8c). Lavas with anomalously low $\delta^{18}O$ coarse olivine phenocrysts are only found in subaerial Mauna Kea lavas, which fall only on the "Low-8" array. This result suggests that the Pb isotope composition of a low-$\delta^{18}O$ component contributing to Hawaiian lavas has a $^{206}Pb/^{204}Pb$ ratio of ~18.4 to 18.5 and falls on or

below the Low-8 array in Figure 8c. This is less radiogenic, but similar in $^{208}Pb^*/^{206}Pb^*$, to the composition suggested for the Kea component by *Eiler et al.* [1996b]. *Eisele et al.* [2003] suggest that the highest $^{206}Pb/^{204}Pb$ ratios in Figure 8c, where all three Pb isotope arrays converge, are a signature of recycled oceanic crust in the Hawaiian plume. There are no samples with low-$\delta^{18}O$ phenocrysts at these most radiogenic compositions, suggesting that this component is not the cause of low $\delta^{18}O_{olivine}$ values. Similarly, several articles in this theme [*Blichert-Toft et al.*, 2003; *Eisele et al.*, 2003; Kurz, submitted manuscript, 2003; *Feigenson et al.*, 2003] suggest that relatively thorogenic Pb isotope compositions (the ''High-8'' array) are a distinctive property of a plume component. Our data provide no evidence that this signature is associated with low $\delta^{18}O_{olivine}$ values. *Eisele et al.*'s [2003] ''Low-8'' Pb isotope array—a signature that does appear to be associated with low $\delta^{18}O_{olivine}$ values—is not discussed at length in other articles in this theme. However, both *Feigenson et al.* [2003] and *Huang and Frey* [2003] suggest that it is associated with relatively low degrees of melting of the edges of the Hawaiian plume, the composition of which might be influenced by the upper-mantle sources of MORBs.

4. Discussion

4.1. Evaluation of the Effects of Aqueous Alteration

[27] Differences in $\delta^{18}O$ between fine and coarse grains of the same mineral (Figures 1c and 2) and deviations of interphase fractionations from high-temperature equilibrium (Figure 3) can be characteristic of weathered or hydrothermally altered rocks [*Ryerson et al.*, 1989; *Gazis et al.*, 1996; *Holt and Taylor*, 1998]. On the other hand, Puu Oo lavas are unambiguously unaltered—many were collected minutes to hours after eruption—and are also characterized by microphenocrysts with $\delta^{18}O$ values lower than coarse olivine phenocrysts from other Kilauea lavas [*Eiler et al.*, 1996b; *Garcia et al.*, 1998] and by olivine-glass fractionations that are ~0.5‰ out of equilibrium [*Garcia et al.*, 1998]. Therefore at least some Hawaiian lavas undergo magmatic processes that produced oxygen isotope systematics like those we observe for HSDP-2 samples.

[28] Several lines of evidence suggest the variations we observe in the HSDP-2 core reflect magmatic rather than subsolidus processes: (1) Individual samples, and in some cases even entire stratigraphic units, are nearly homogeneous in $\delta^{18}O$ for any one phase (e.g., olivine phenocrysts in the submarine section); (2) stratigraphic variations in $\delta^{18}O$ are subtle (~1‰) and change systematically across major boundaries (e.g., the Mauna Loa/Mauna Kea contact); and (3) most (eight of eleven) measured fractionations between glass and microphenocrysts closely conform to high-temperature equilibrium. In contrast, weathering and hydrothermal alteration typically produce shifts in $\delta^{18}O$ of many per mil, heterogeneity on all scales (from individual grains to many meters), and departures from high-temperature equilibrium fractionation that are largest for the most susceptible materials like glass and fine-grained minerals [e.g., *Gazis et al.*, 1996; *Holt and Taylor*, 1998; *Valley and Graham*, 1993; *Eiler et al.*, 1995]. Finally, (4) values of $\delta^{18}O$ in the HSDP-2 core are uncorrelated with minor-element indices that are sensitive to aqueous alteration (e.g., Rb/Ba, Rb/K, and K_2O/P_2O_5 [see *Huang and Frey*, 2003]).

4.2. Relationships Between Phenocrysts and Host Lavas

[29] Most coarse olivine phenocrysts in HSDP-2 lavas are in some sense xenocrystic because they have oxygen isotope compositions out of equilibrium with their host lavas. These grains are also usually too forsterite-rich to be in Fe/Mg exchange equilibrium with their host lavas and often contain kink-bands, suggesting they resided in cumulate piles prior to entrainment in their host lavas—both observations that have been used to suggest they are xenocrysts [e.g., *Clague et al.*, 1995; *Baker et al.*, 1996]. However, when interpreting the isotopic compositions of these grains, it is important to distinguish between two possibilities: (1) Hawaiian magmas might vary in $\delta^{18}O$ over the course of their crystallization-differentiation history, such that early formed olivine phenocrysts record one point

in that evolution and late-formed phenocrysts and matrix another point. In this case, the coarse, magnesian olivine crystals are related to their host lavas even if they are not in isotopic equilibrium with them at the time of eruption. (2) Alternatively, coarse, magnesian olivine crystals might have precipitated from an unrelated magma in the volcanic edifice and later been entrained in their host lavas prior to eruption; in this case, coarse olivine crystals have no direct relationship to host lavas. Correlations between the $\delta^{18}O$ of olivine phenocrysts and lithophile-element geochemistry of host lavas provide one means of testing between these alternatives. The existence of such correlations in Figures 7a–7d suggest the first of these alternatives is the case (note that similar arguments apply to the interpretation of Os and He isotope data, which are dominated by coarse olivine crystals [Kurz, submitted manuscript, 2003; *Lassiter and Hauri*, 1998]).

4.3. Oxygen Isotope Fractionation During Crystallization and Partial Melting

[30] Figures 2, 3, and 7e provide evidence that processes of crystallization-differentiation are associated in some way with variations in $\delta^{18}O$. In this section we ask whether these variations could be caused by high-temperature, equilibrium fractionations between crystals and melt. *Eiler* [2001] shows that crystallization of olivine ± spinel leads to subtle increases in $\delta^{18}O$ values of residual basaltic melts (~0.1‰ for ~20% crystallization); further cotectic crystallization of olivine plus clinopyroxene and/or plagioclase leads to minimal additional changes in $\delta^{18}O$ until after olivine is no longer a liquidus phase. The approximate predicted trend of $\delta^{18}O$ and other geochemical indices for these models are shown in Figures 7a–7e as dashed arrows pointing in the direction of increasing extent of crystallization. These predicted changes are nearly orthogonal to observed trends. Similarly, crystallization-differentiation alone produces increases in $\delta^{18}O$ over the course of differentiation; therefore it cannot explain the observation in Figures 2 and 3 that olivine microphenocrysts (generally late-formed [*Clague et al.*, 1995]) are lower in $\delta^{18}O$ than olivine phenocrysts (generally early formed [*Clague et al.*, 1995]). We conclude that fractional crystallization may be correlated with processes that change $\delta^{18}O$, but that equilibrium fractionations between solid and melt are not the cause of those relationships.

[31] Magmas parental to HSDP-II lavas were generated by a range of extents of melting of their mantle sources, and there are statistically significant correlations between $\delta^{18}O$ values of phenocrysts and geochemical indices that are sensitive to extent of melting (e.g., Sm/Yb, Al_2O_3/TiO_2; V/Ti could also vary with extent of melting; Figures 7a–7c and 8a). Therefore we consider whether high-temperature equilibrium fractionations between melts and residual solids during partial melting could generate the oxygen isotope variations we observe. *Eiler* [2001] shows that partial melting of lherzolites can generate a total range in $\delta^{18}O$ of product melt of only 0.10‰ over the course of up to 30 wt.% partial melting. The correlations between $\delta^{18}O$ and other geochemical indices predicted by such calculations are shown in Figures 7a–7e as solid arrows pointing in the direction of increasing extent of melting. These model predictions are obviously at odds with the trends we observe. Moreover, fractionations accompanying partial melting would not be expected to generate systematic isotopic differences between olivine phenocrysts and microphenocrysts (Figure 2). We conclude that partial melting of isotopically homogeneous peridotite is incapable of producing the oxygen isotope variations we observe.

4.4. Possible Sources of Low-$\delta^{18}O$ Components

[32] The preceding discussion establishes that the oxygen isotope stratigraphy of the HSDP-2 core principally reflects differences in $\delta^{18}O$ among the mantle sources and/or lithospheric contaminants of Hawaiian lavas rather than subsolidus alteration, fractional crystallization and/or partial melting. In this section we discuss amounts and identities of components that could have led to these oxygen isotope variations.

[33] Most mantle rocks and mantle-derived magmas span a narrow range in $\delta^{18}O$ that we have referred to as "normal" throughout preceding

sections of this paper (i.e., $\delta^{18}O_{olivine}$ between ~5.0 and 5.2‰, or $\delta^{18}O_{melt}$ of 5.4 to 5.6‰ [*Eiler*, 2001]). Because a wide range of ultramafic rocks have $\delta^{18}O$ values in this range, little specific is implied about the mantle sources of basalts that also have such values, other than that they lack recycled crustal materials in abundances greater than a few percent. However, where values outside this range are observed, they provide relatively specific constraints on the origin and amounts of isotopically anomalous materials in the sources of those lavas. In this context, the important finding of this study is that olivine phenocrysts in subaerial Mauna Kea lavas and both olivine microphenocrysts and host glass or matrix throughout Mauna Kea are lower in $\delta^{18}O$ than this "normal" range.

[34] The only major earth reservoir known to have a $\delta^{18}O$ value significantly less than average mantle is the hydrosphere, and rocks only take on this value as a result of high-temperature water-rock interaction. The greatest volume of low-$\delta^{18}O$ rocks produced by this process are in the oceanic lithosphere, which undergoes extensive hydrothermal alteration at ridges [*Shanks*, 2001]. These low-$\delta^{18}O$ signatures persist long after the lithosphere has cooled [*Gregory and Taylor*, 1981]. Furthermore, there is evidence that these signatures survive subduction and are mixed into the mantle [*Garlick et al.*, 1971]. It is poorly known, but important to our discussion, how deep in the ocean lithosphere low-$\delta^{18}O$ rocks exist. These compositions are common in the gabbroic portions of most characterized sections of ocean crust [*Muehlenbachs*, 1986], but it is unclear whether ultramafic rocks beneath the petrologic MOHO are also commonly low in $\delta^{18}O$. On one hand, permeabilities decrease dramatically at these depths and limit fluid infiltration [*Walther and Orville*, 1982], so low $\delta^{18}O$ values are not expected. On the other hand, some ophiolites contain low $\delta^{18}O$ ultramafic rocks that could have acquired their oxygen isotope signatures before obduction [*Miller et al.*, 2001], so aqueous alteration might penetrate deep in the ocean lithosphere despite expectations. Finally, active volcanoes frequently support meteoric hydrothermal systems, particularly in portions of their edifices having extensional structures. These systems are believed to be the principle sources of ^{18}O-depleted crustal contaminants responsible for low $\delta^{18}O$ values in Icelandic lavas [e.g., *Eiler et al.*, 2000c], and have been proposed as a contributor to (although perhaps not the only cause of) low $\delta^{18}O$ values in recent Kilauea lavas [*Garcia et al.*, 1998].

[35] A key aspect of all low-$\delta^{18}O$ components is that they must be sampled in large mass fractions to produce measurable decreases in the $\delta^{18}O$ of basaltic lavas. For example, the contrast between even the lowest-$\delta^{18}O$ portions of the oceanic lithosphere (~0‰) and average mantle is only ~5‰, and thus lavas must sample at least 10% of such materials as subducted components of their mantle sources or as shallow-level contaminants in order to reach $\delta^{18}O_{olivine}$ values of ~4.5‰. Hydrothermally altered rocks in subaerially exposed volcanic edifices can be lower in $\delta^{18}O$ than 0‰ (down to ~−5 to −10‰) due to the influence of low-$\delta^{18}O$ meteoric water and boiling processes; in these cases, proportionally smaller amounts of contamination (i.e., ~6 to 3%, respectively) would be required to produce measurable shifts in the $\delta^{18}O$ of erupted lavas.

4.5. Link Between Crystallization and the Abundance of Low-$\delta^{18}O$ Component(s)

[36] Two key features of our results are (1) the abundance of the low-$\delta^{18}O$ component led not only to variations in $\delta^{18}O$ of erupted lavas but also to oxygen isotope disequilibrium between components of those lavas (Figures 1c, 2, and 3), and (2) $\delta^{18}O$ values of glasses (Figure 7e) and perhaps phenocrysts (Figure 7c) are correlated with chemical indices that are sensitive to crystallization-differentiation. In this section, we propose a model that quantitatively explains these observations as consequences of progressive addition of low-$\delta^{18}O$ component (whatever its origin) to Hawaiian magmas over the course of their crystallization-differentiation.

[37] Figure 9 summarizes the essential features of our model, including the extent of crystallization and identity of phases crystallizing from primary basaltic magma parental to HSDP-2 lavas (Figure 9a; calculated using the MELTs algorithm, assuming the *Baker et al.* [1996] estimate for primary Mauna

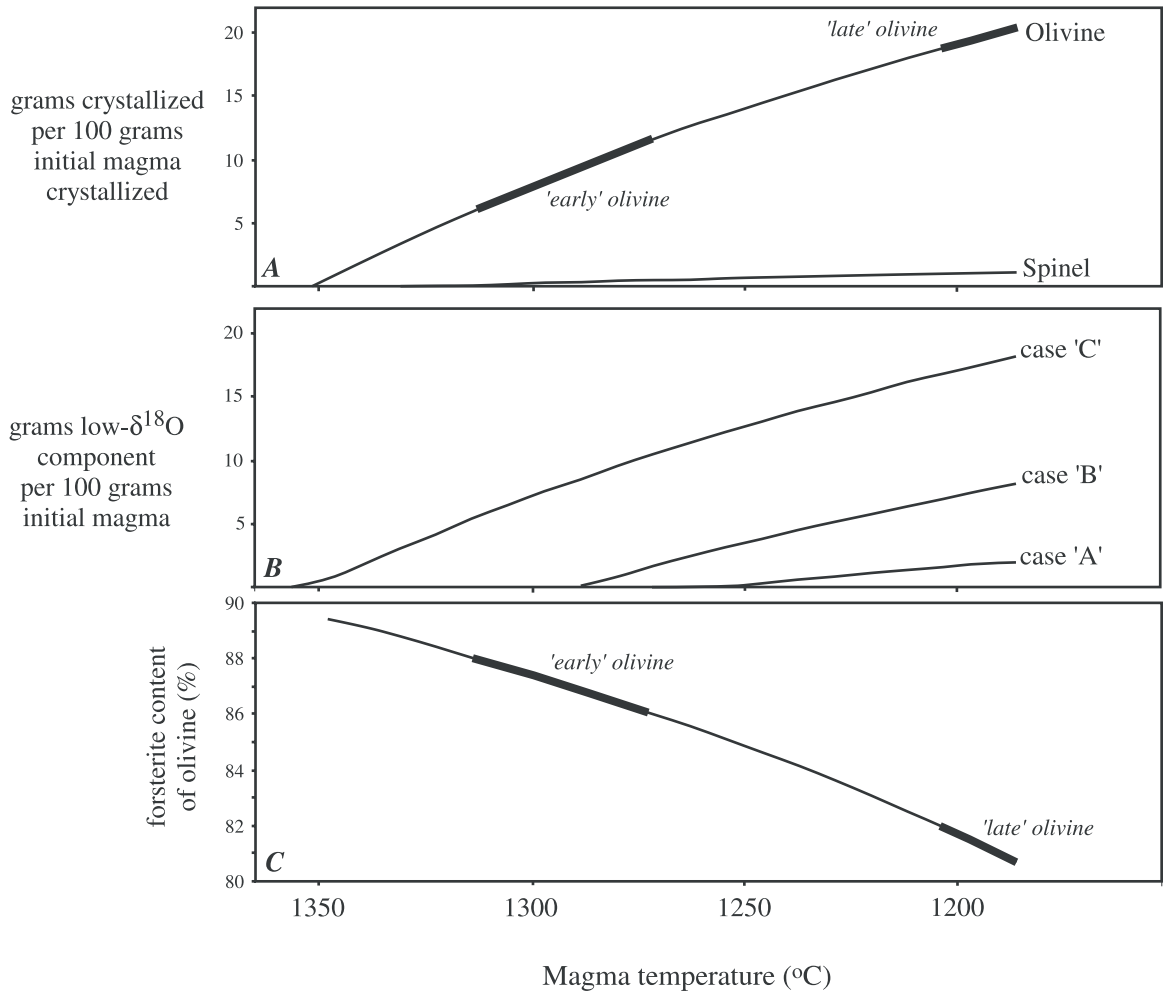

Figure 9. Outline of the essential features of our proposed model for simultaneous crystallization-differentiation and mixing with a low-$\delta^{18}O$ component. Amounts, identities and mineral-chemistries of crystallizing phases are calculated using the MELTs algorithm [*Ghiorso et al.*, 1994] assuming an initial Mauna Kea magma given by *Baker et al.* [1996]. Amounts of low-$\delta^{18}O$ component added over the course of crystallization-differentiation are prescribed for each of three cases (A, B, and C), as shown. Heavy line segments in panels A and C show the populations of "early" and "late" olivine we consider as approximate model predictions for phenocrysts and microphenocrysts, respectively.

Kea magma, a pressure of 1000 bars and oxygen fugacity controlled by the QFM buffer), the amount of low-$\delta^{18}O$ component mixed into that magma during its crystallization-differentiation (Figure 9b; assuming several representative cases detailed below), and the Mg# of olivine grown from that magma at any point in the differentiation/mixing process (Figure 9c; based on output of the calculated fractionation-crystallization path for primary Mauna Kea magma illustrated in Figure 9a). For the purposes of simplicity, we assume that the low-$\delta^{18}O$ component is mafic in composition, so that it does not substantially dilute the MgO content of basaltic magmas into which it is mixed. All three variables are plotted versus model magmatic temperature (decreasing to the right), which is a useful proxy for order of increasing extent of differentiation.

[38] Systems undergoing processes of combined crystallization and mixing can vary in relative timing of the two processes and in the total amount of admixed component. To illustrate such variations, we show three cases: addition of low $\delta^{18}O$ component is small in extent and begins late in the history of olivine crystallization (case A); addition of low-$\delta^{18}O$ component is moderate in extent and

begins after approximately half the crystallizing assemblage has precipitated (case B); and addition of low-$\delta^{18}O$ component is large in extent and begins early in the history of olivine crystallization (case C). Other combinations are possible; these were chosen because they are plausible and, as is shown below, lead to a range of oxygen isotope systematics that resembles our data. We assume that the maximum amount of low-$\delta^{18}O$ component that can be added in case C is controlled by the heat budget of a system undergoing assimilation/fractional crystallization (i.e., the latent heat of fusion of mafic, low-$\delta^{18}O$ component is less than or equal to the latent heat of crystallization of the precipitating assemblage plus the specific heat change of cooling magma). However, this limit need not apply to systems in which the heat liberated by one generation of magmas contributes to melting contaminants that are mixed into another generation of magmas [*Bergantz*, 1989]. Thus larger amounts of low-$\delta^{18}O$ component could be added even if it is a lithospheric contaminant.

[39] The important feature of this model is that both olivine crystallization and addition of low-$\delta^{18}O$ component take place gradually and simultaneously. As a result, the first-formed olivine grows from magma containing less low-$\delta^{18}O$ component than does the last-formed olivine, and, assuming early formed olivine cannot isotopically re-equilibrate with host magma (reasonable given the slow rates of oxygen self diffusion in olivine [*Ryerson et al.*, 1989]), only the last olivine to crystallize is in oxygen-isotope equilibrium with the erupted host lava. For the purposes of discussion and comparison with our data, we discriminate between two populations of olivine that form at different stages of the model differentiation process: ''early'' olivines having forsterite contents of 88 to 86% and ''late'' olivines having forsterite contents of 82 to 80%. These two populations are marked in Figures 9a and 9c as heavy black line segments. The ''early'' olivines were chosen to have forsterite contents comparable to those of the most abundant coarse olivine phenocrysts in Hawaiian lavas [*Clague et al.*, 1995; *Baker et al.*, 1996] (Table 2) and reasonably represent the predictions of our model for phenocryst data (Figure 1a). The ''late'' olivines were chosen to have forsterite contents comparable to those of skeletal, equant and resorbed microphenocrysts in Hawaiian lavas [*Clague et al.*, 1995; *Baker et al.*, 1996] (Table 2) and reasonably represent the predictions of our model for microphenocryst data (Figure 1c; Table 2).

[40] By assigning $\delta^{18}O$ values to the primary melt and the low-$\delta^{18}O$ component, and by adopting existing constraints on oxygen isotope fractionations associated with olivine crystallization [*Eiler*, 2001], the model outlined in Figure 9 predicts the differences in $\delta^{18}O$ between early and late formed phenocrysts, between phenocrysts and final (i.e., post-differentiation) host melt, and the relationship between melt—phenocryst fractionations and the amount of low-$\delta^{18}O$ component added, and the relationship between MgO and $\delta^{18}O$ in erupted melt. We adopted values of 5.5‰ for primary melt (equal to the $\delta^{18}O$ of normal MORBs and similar to the matrix of a Mauna Loa lava analyzed in this study) and a value of 0‰ for the low-$\delta^{18}O$ component. This value is at the lower end of the range for hydrothermally altered mafic and ultramafic rocks near the base of the oceanic crust [*Muehlenbachs*, 1986; *Miller et al.*, 2001] and their subducted equivalents [*Garlick et al.*, 1971], and is within the range expected for hydrothermally altered rocks in Kilauea's east rift

Figure 10. (opposite) Comparison of our observations with the predictions of the model outlined in Figure 9, assuming initial melt has a $\delta^{18}O$ of 5.5‰ (comparable to NMORBs and in equilibrium with typical olivine in oceanic basalts [*Eiler*, 2001]) and the low-$\delta^{18}O$ component has a $\delta^{18}O$ of 0‰ (at the lower end of the range for hydrothermally altered oceanic lithosphere and its subducted equivalents and within the range possible for materials in the Hawaiian volcanic edifice). Figure 10a plots our model predictions in the same way data is plotted in Figure 3. Black squares show model predictions for ''early'' olivine for cases A, B and C (as labeled). The black arrow shows the predicted change in $\delta^{18}O$ of melt and coexisting, equilibrated olivine with increasing amounts of differentiation and mixing; italicized letters show the locations on that line of predictions for ''late'' olivine for cases A, B and C. Figure 10b plots our model predictions in the same was data is plotted in Figure 7e. In this case, model predictions for melt are shown for cases A, B and C (as labeled). In both cases, gray symbols reproduce data from Figures 3 and 7e, respectively.

zone [*Garcia et al.*, 1998]. Thus it is a single model value that provides reasonable predictions regardless of the source (plume, lithosphere, or edifice) of low-$\delta^{18}O$ component. In reality, a range of $\delta^{18}O$ values is expected of any of the possible low-$\delta^{18}O$ components, and this model is expected to fit only the directions and approximate magnitudes of observed trends and ranges.

[41] Figure 10a illustrates our model's predictions for the locations of "early" and "late" olivines on a plot of $\delta^{18}O_{olivine}$ versus $\delta^{18}O_{melt}$. This figure is

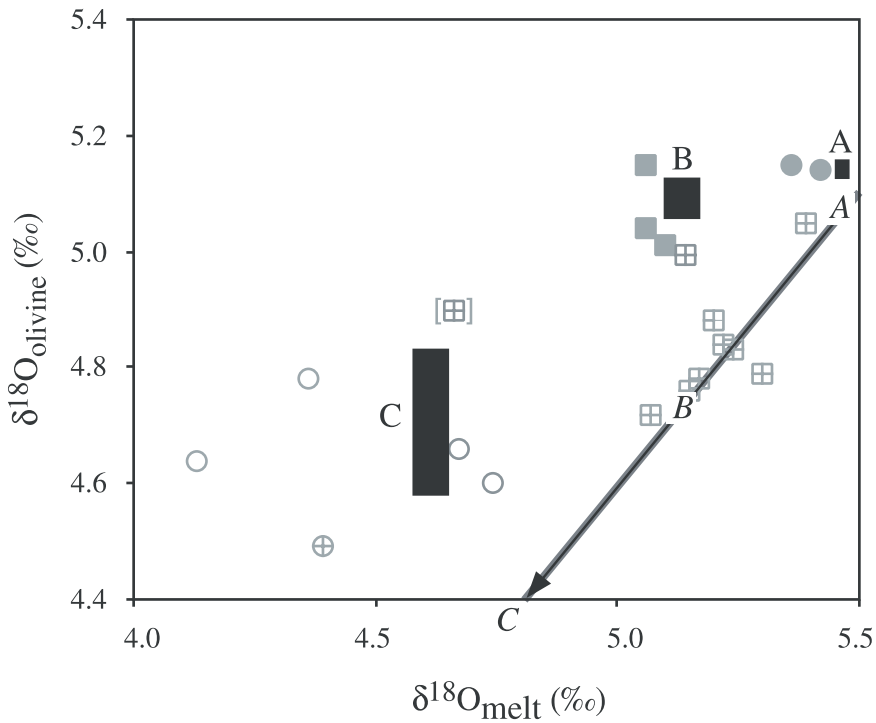

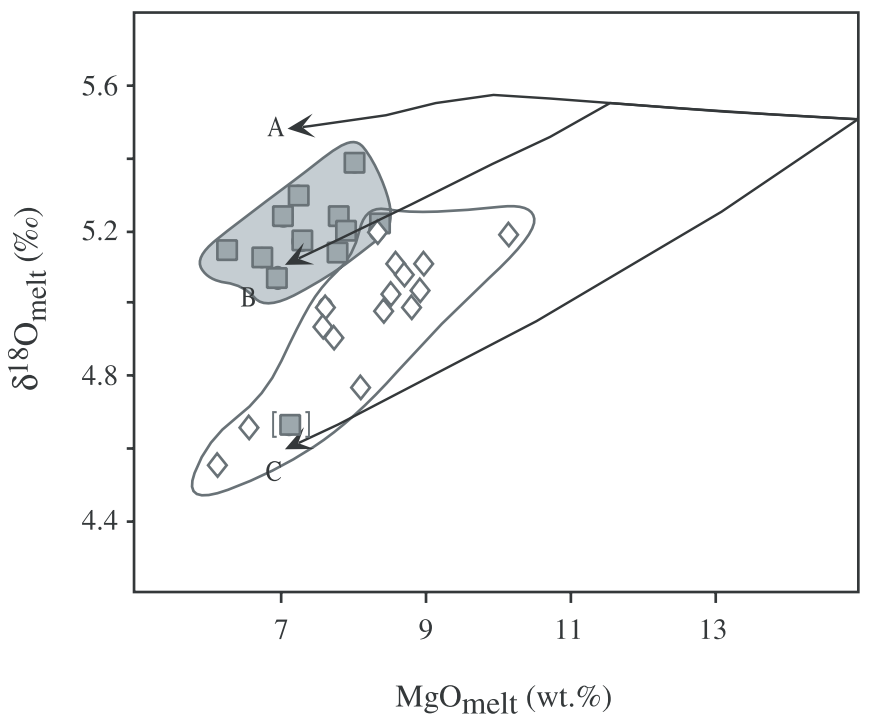

plotted at the same scale as Figure 3 and data from Figure 3 are reproduced as faint gray symbols. Ranges predicted for "early" olivines in case A (minor mixing), B (moderate mixing) and C (extensive mixing) are shown as black boxes and labeled according to the model case they represent. "Late" olivines are always predicted to fall on or near the equilibrium line of slope 1; italicized letters mark the predicted locations on that line for cases A, B and C. Our model quantitatively reproduces all the first-order features of our data: phenocrysts, like model "early" olivine, fall above and to the left of the equilibrium line, and are further from that line in low-$\delta^{18}O_{melt}$ lavas than in high-$\delta^{18}O_{melt}$ lavas (i.e., the lowest $\delta^{18}O$ phenocrysts are preferentially found in exceptionally low-$\delta^{18}O$ hosts). This latter detail is predicted by our model but would not be expected if phenocrysts were accidental xenocrysts that crystallized from higher-$\delta^{18}O$ magmas unrelated to their host. Furthermore, most microphenocrysts, like model "late" olivine, fall on the equilibrium line and are ~0.2‰ lower in $\delta^{18}O$ than phenocrysts from related lavas (we presume the few exceptions are small olivine grains that we classified as microphenocrysts but are not the last olivines to grow from their host). Finally, the difference in $\delta^{18}O$ between early and late olivines is expected to increase as the $\delta^{18}O$ of host melt decreases—also consistent with the data in Figure 3.

[42] Figure 10b illustrates our model's predictions for the relationships between $\delta^{18}O$ and MgO of melt over the course of combined crystallization-differentiation and mixing with low-$\delta^{18}O$ component; lines for cases A, B and C are marked. Data for Mauna Kea and Puu Oo glasses are reproduced from Figure 7e as faint gray symbols; fields surround each data set for added clarity. Figure 10b covers a broader scale than Figure 7e in order to encompass model predictions for more primitive glasses that might eventually be found and analyzed for $\delta^{18}O$. As in Figure 10a, model trends provide a satisfactory explanation for the observed trends. In detail, model B appears to provide the best fit to data for submarine Mauna Kea lavas (as in Figure 10a), whereas cases intermediate between models B and C appear to provide better fits to data from Puu Oo and the anomalous submarine Mauna Kea sample, SR0698-5.6 (as is the case for that sample and subaerial Mauna Kea samples in Figure 10a).

[43] We conclude on the basis of the preceding discussion that the addition of low-$\delta^{18}O$ component to magmas parental to HSDP-2 lavas was gradual and took place while they were undergoing fractional crystallization of olivine. This is a powerful constraint on the origin of the low-$\delta^{18}O$ component and the processes by which it was sampled because of the limited depth range over which Hawaiian basalts undergo crystallization-differentiation. Oceanic intraplate basalts generally differentiate within the lithosphere. It has been argued that they often do so at pressures of ~10 to 20 kb (~35–70 km depth, or within the lower lithospheric mantle) based on the importance of clinopyroxene fractionation in their differentiation [*Albarede*, 1992]. However, Hawaiian tholeiites generally lack clear evidence of clinopyroxene fractionation [e.g., *Clague et al.*, 1995; *Huang and Frey*, 2003]. Their differentiation is instead dominated until its latest stages by olivine. Fluid-inclusion barometry indicates that this olivine generally forms at pressures less than or equal to ~5 kb (~15 km—approximately the depth to the MOHO beneath Mauna Kea [e.g., *Reoder*, 1965]). *Anderson and Brown* [1993] suggest on the basis of CO_2 contents of olivine-hosted melt inclusions that most olivine crystallization takes place at pressures near 2 kb. This corresponds to a depth of ~5 to 6 km—within the volcanic edifice of a fully grown Hawaiian volcano or perhaps within the underlying Cretaceous crust in a younger and smaller one. In light of these arguments, our data appear to require that the low-$\delta^{18}O$ component (whatever its origin) was added to HSDP-2 magmas while they resided in the upper portions of the Cretaceous lithosphere (approximately at or above the MOHO) and/or the volcanic edifice.

5. Summary and Conclusions Regarding the Petrogenesis of Low-$\delta^{18}O$ HSDP-II Lavas

[44] The most significant interpretations we put forward in preceding sections are summarized

and briefly elaborated upon in the following paragraphs:

[45] • Oxygen isotope compositions of handpicked olivine, glass and groundmass from HSDP-II lavas, including interphase fractionations, largely or entirely reflect magmatic rather than subsolidus processes and are not dominantly controlled by high-temperature equilibrium fractionations accompanying partial melting and/or crystallization-differentiation. Those compositions can reflect mixing between magmas having normal $\delta^{18}O$ and magmas and/or assimilants having anomalously low $\delta^{18}O$. Candidates for the low-$\delta^{18}O$ component include hydrothermally altered oceanic lithosphere in the Pacific plate, subducted fragments of hydrothermally altered oceanic lithosphere entrained in the Hawaiian plume, or hydrothermally altered components of the Hawaiian volcanic edifice.

[46] • The low-$\delta^{18}O$ component(s) was added over the course of crystallization-differentiation of higher-$\delta^{18}O$ magma. This restricts the mixing process to depths within ~15 km of the surface—the depth interval of olivine crystallization.

[47] • Low-$\delta^{18}O$ component is present but low in abundance and only detectable in late-stage differentiation products (i.e., glass and microphenocrysts, but not coarse, magnesian phenocrysts) in submarine Mauna Kea lavas. In contrast, the low-$\delta^{18}O$ component is high in abundance and detected in the earliest differentiation products throughout subaerial Mauna Kea lavas.

[48] • Anomalously low-$\delta^{18}O$ olivine phenocrysts appear suddenly at the subaerial/submarine transition in Mauna Kea. This sharp transition is mirrored by a change in the distribution of fractionation-normalized SiO_2 contents (from bimodal in the submarine section to unimodal in the subaerial section).

[49] • Low-$\delta^{18}O$ signatures are correlated with other geochemical indices that are associated with low-degree melting of upper mantle and/or lithosphere on the margins of the Hawaiian plume [*Huang and Frey*, 2003; *Blichert-Toft et al.*, 2003; *Chen and Frey*, 1983]. Most such correlations are defined by the contrast between average compositions of subaerial and submarine Mauna Kea lavas (Figures 7a–7d and 8); in this case, we believe these correlations could reflect either unique geochemical properties of a low-$\delta^{18}O$ component, or a coincidence that a low-$\delta^{18}O$ component is sampled in greater abundance at the same time that primary magmas are changing in composition for other reasons. In addition, an interval of the submarine Mauna Kea section (between 2150 and 2350 mbsl) records correlated stratigraphic trends in $\delta^{18}O$ and various radiogenic isotope ratios (Figure 6); this observation suggests that low-$\delta^{18}O$ values are derived from a component with relatively MORB-like geochemistry that can be present at any time in Mauna Kea's evolution.

[50] • There is no evidence that anomalously low $\delta^{18}O$ values are associated with highly anomalous, presumably plume-derived radiogenic isotope compositions (i.e., high $^{208}Pb^*/^{206}Pb^*$, $^3He/^4He$, and $^{87}Sr/^{87}Sr$; low ε_{Nd} and ε_{Hf}).

[51] Our results are difficult to reconcile with the interpretation that low $\delta^{18}O$ values in Hawaiian lavas are derived from a component of the Hawaiian plume [*Harmon and Hoefs*, 1995; *Lassiter and Hauri*, 1998; *Hauri*, 1996; *Blichert-Toft et al.*, 1999]. In particular, it is difficult to envision why a low $\delta^{18}O$ source component would be sampled in increasingly larger amounts over the course of low-pressure crystallization-differentiation. Furthermore, one would expect lavas rich in low-$\delta^{18}O$ component, if it consists of ancient, recycled lithosphere, to have exotic radiogenic isotope compositions (e.g., high $^{206}Pb/^{204}Pb$ [*Eisele et al.*, 2003]) rather than the observed modest shifts toward compositions resembling modern MORBs. Finally, the only positive evidence previously cited for the plume origin of this component was based on it having a lower ε_{Hf} value than normal MORBs [*Blichert-Toft et al.*, 1999]. However, *Kempton et al.* [2000] and *Chauvel and Blichert-Toft* [2001] recently showed that Pacific MORBs are unusually low in ε_{Hf}, ranging down to values similar to Mauna Kea lavas (i.e., Hf isotope data alone are consistent with local asthenosphere, local lithosphere, or the plume as sources of the

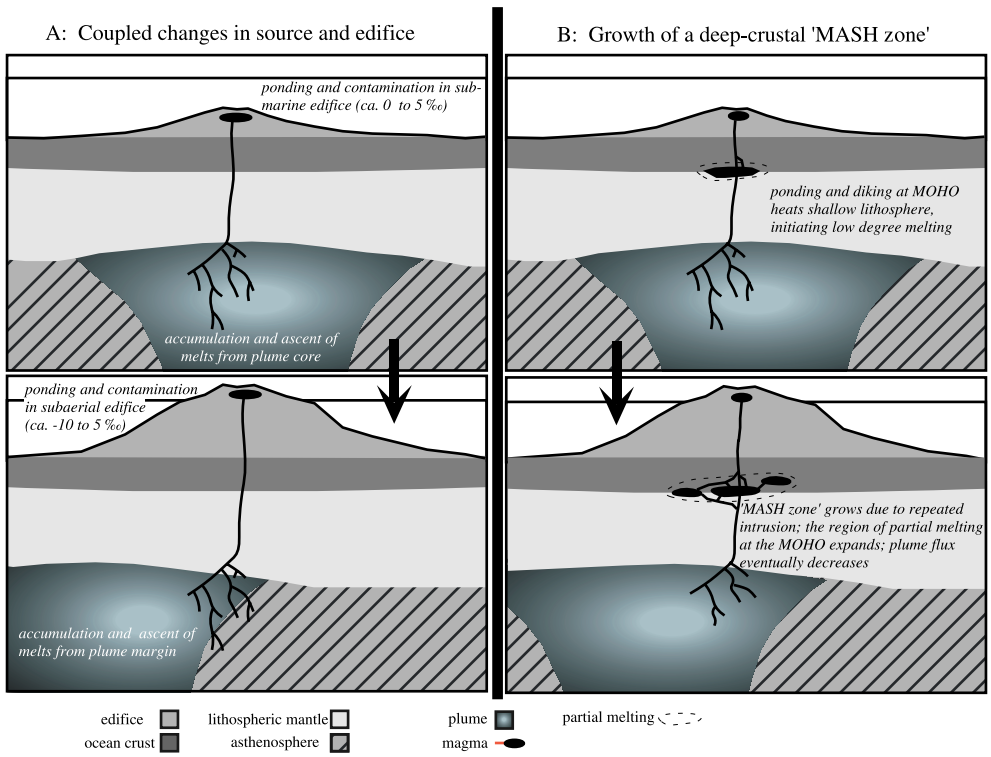

Figure 11. Cartoons illustrating two proposed models for the temporal evolution of Mauna Kea that are consistent with the oxygen isotope geochemistry and other geochemical properties of its lavas. In the first model (A; the top panel shows an early stage of the volcano's evolution and the bottom panel shows the end of shield-building volcanism), aging of the volcano is associated with two processes: increasing proportions of low-degree melt from the cool outer margins of the plume (the composition of which is influenced by mixing with upper mantle) and/or the lithospheric mantle, and simultaneously increasing amounts of contamination by low-$\delta^{18}O$ volcanic edifice in the subaerial rift zones through which magmas pass. According to this model, correlations between $\delta^{18}O$ and other geochemical properties (e.g., Figures 6, 7, and 8) are fortuitous or result from the fact that both processes are increasingly important over the same span of the volcano's life. In the second model (B; the top panel shows an early stage of the volcano's evolution and the bottom panel shows the end of shield-building volcanism), low degree melt of the shallow lithosphere is generated in a "MASH zone" near the petrologic MOHO [*Hildreth and Moorbath*, 1988]. The proportional contribution of that melt to erupted lavas increases with time as a result of gradual heating of the "MASH-zone" by repeated intrusion combined with decreased magma flux as the volcano drifts off the plume axis. Both models are consistent with existing constraints but have advantages and disadvantages. The first calls on processes known to occur in the shallow plumbing systems of Hawaiian volcanoes [*Garcia et al.*, 1998] but requires special pleading to produce geochemical trends (Figures 6 through 8). The second explains these geochemical trends but calls on a process that is little explored in oceanic intraplate settings, and requires a significant fraction of olivine crystallization occurs at great depths (~10–15 km).

low-$\delta^{18}O$ component). Therefore, while we recognize that one could construct a model describing our results in terms of a low-$\delta^{18}O$ plume component, there is no evidence clearly in favor of this hypothesis and several observations appear to argue against it. We instead focus our attention on two models involving contamination in the lithosphere or volcanic edifice, which we think can more plausibly explain a wider range of our data. These models are schematically illustrated in Figure 11 and explained in the following paragraphs:

5.1. Coupled Evolution of Mantle Sources and Shallow Volcanic Plumbing (Figure 11a)

[52] The end of Mauna Kea's period of shield building volcanism could have involved two temporal trends: (1) gradually increasing contributions

of a "normal"-$\delta^{18}O$, low-degree melt of the asthenosphere and/or lithospheric mantle beneath Hawaii as the volcano moved away from the plume axis [*Huang and Frey*, 2003; *Feigenson et al.*, 2003] and (2) gradually increasing degrees of contamination by low-$\delta^{18}O$ rocks in the volcanic edifice, such as occurs today in Kilauea's east rift zone [*Garcia et al.*, 1998]. These two different processes need not be correlated with one another, but one can imagine how they could be. As the volcano grows and ages, it moves off the plume axis and taps greater proportions of low degree melts from the plume edges. Simultaneously, the edifice gets larger so that subaerially exposed rift zones and their low-$\delta^{18}O$ hydrothermal systems make up more of their upper several kilometers. Thus the population of lavas tapping the largest proportion of source components from the plume edges or the over-riding plate will be exposed to the lowest-$\delta^{18}O$ rocks in the volcanic edifice through which they erupt.

[53] This hypothesis provides an explanation for evidence that low-$\delta^{18}O$ component is added to Mauna Kea magmas gradually over the course of their differentiation (Figures 2 and 7e) because the heat required to melt crustal assimilants is expected to be, in part, balanced by the latent heat of crystallization of phenocrysts [e.g., *Aldanmaz et al.*, 2000; *Bindeman and Valley*, 2001] and the low-$\delta^{18}O$ component is only available in the crustal environments where most crystallization takes place. It also provides an explanation for why the subaerial/submarine transition is a sharp break in oxygen isotope composition of phenocrysts (Figure 1a) but only roughly coincides with the start of gradual changes in radiogenic isotope and trace element geochemistry (Figure 4): The lower limit in $\delta^{18}O$ of hydrothermally altered rocks in submarine volcanoes is $\sim$0‰ (the value for seawater), whereas subaerial volcanoes can contain hydrothermally altered rocks with $\delta^{18}O$ values down to ~ -10 to -15‰ caused by interaction with meteoritic precipitation and products of low-pressure boiling processes [*Garcia et al.*, 1998, and references therein]. Thus the change in $\delta^{18}O$ across the subaerial/submarine transition in Mauna Kea could reflect a sudden increase in the contrast in $\delta^{18}O$ between its primary magmas and hydrothermally altered rocks in its volcanic edifice. Finally, this model could help understand the change in modality of fractionation-normalized SiO_2 contents across the subaerial/submarine transition (Figure 5). Stolper et al. (submitted manuscript, 2003) suggest that intermediate SiO_2 magmas could be mixtures of the high- and low-SiO_2 magmas that define the bimodal population that dominates the submarine section. Furthermore, they note that intermediate SiO_2 submarine glasses are always degassed and suggest this might signify that magma mixing only takes place in high-level crustal magma chambers. If so, the drop in $\delta^{18}O$ and shift in modality of SiO_2 contents could indicate that the submarine/subaerial transition coincides with the establishment of long-lived, shallow crustal magma reservoirs where mixing, degassing and assimilation take place before eruption. Note, however, that submarine hyaloclastites presumably formed by subaerial eruptions that broke apart at the shore (i.e., they too erupted through shallow magma reservoirs [*Moore*, 2001]), and thus it is hard to understand why there are no hyaloclastites with anomalously low-$\delta^{18}O$, coarse olivine phenocrysts typical of subaerial Mauna Kea lavas (Figure 1a).

[54] If the model illustrated in Figure 11a is correct, low-$\delta^{18}O$ lavas are evidence for the passage of magmas through hydrothermally active parts of their volcanic edifices and thus they provide insight on the past volcanology and hydrology of Hawaii. The broadest, consistent feature of oxygen isotope variations among Hawaiian lavas is that those from Kea trend volcanoes (Kilauea, Mauna Kea, Kohala and Haleakala) are often lower in $\delta^{18}O$ than typical terrestrial basalts whereas those from Loa trend volcanoes (Loihi, Mauna Loa, Hualalai, Lanai, Koolau, and perhaps Kauai) are not. Previously, this difference has been interpreted to reflect greater contributions to magmas parental to "Kea trend" lavas of a low-$\delta^{18}O$ source component in the Hawaiian plume or over-riding Cretaceous Pacific lithosphere [*Eiler et al.*, 1996b; *Lassiter and Hauri*, 1998]. If, instead, low $\delta^{18}O$ values are acquired during their transit through the volcanic edifices through which they erupt, the systematic difference in $\delta^{18}O$ between the Loa

and Kea lavas requires a different explanation. One simple possibility is that Kea trend volcanoes have abundant low-$\delta^{18}O$, hydrothermally altered rocks within their volcanic edifices during their subaerial evolution whereas Loa trend volcanoes do not. This difference could be a consequence of the fact that the northeast sides of the Hawaiian islands receive more rain than their southwest sides (i.e., so vigorous hydrothermal systems are only present in rift zones trending toward the northeastern shores). However, large parts of Mauna Loa do receive significant amounts of rain, and thus requires that there is a threshold in amount of rainfall, currently not understood, below which vigorous hydrothermal systems cannot develop. A further weakness of this hypothesis is that, except under special circumstances, contamination in volcanic edifices involves minimal contrasts in most geochemical properties between magmas and contaminants (because the latter are solidified and altered equivalents of the former). Therefore this model requires that correlations between $\delta^{18}O$ and various lithophile-element abundance ratios and radiogenic isotope ratios (Figures 6 through 8) are fortuitous.

5.2. A "MASH" Zone Beneath Hawaii (Figure 11b)

[55] The low-$\delta^{18}O$ component could be a low-degree melt of the Cretaceous Pacific crust and/or shallow lithospheric mantle that mixes into Hawaiian magmas as they begin to differentiate at depths near the MOHO. The best analogy with such deep-crustal contamination processes could be the "MASH"-zones ("Melting-Assimilation-Storage-Homogenization") suggested to exist in lower crustal magmatic systems at convergent margins [*Hildreth and Moorbath*, 1988]. These systems are characterized by repeated intrusion of mantle-derived basalt near the MOHO, producing a complex of dikes and sills that heats and partially melts intervening septa of pre-existing lower-crustal and upper mantle rocks. Mixing of these partial melts into the intruding basalts produces hybrid magmas. In continental convergent margins, this process leads to siliceous hybrid magmas because the quartzo-feldspathic crustal rocks produce SiO_2-rich partial melt. In this case, one might expect this process to lead to systematically higher fractionation-normalized SiO_2 in low $\delta^{18}O$ lavas, in contrast with our observations (Figures 1 and 5). However, similar systems active near the oceanic MOHO might instead produce low-degree partial melt of mafic and ultramafic rock types, which could have smaller major-element contrasts with invading plume-derived magmas and thus produce less obvious changes in major element chemistry.

[56] This hypothesis could be consistent with our conclusion that low-$\delta^{18}O$ component was added to Mauna Kea magmas over the course of their differentiation, but only if olivine crystallization occurs at depths within the lithosphere and below the volcanic edifice ($\sim$10 to 15 km). Hawaiian magmas crystallize olivine over a range of depths, the upper end of which is consistent with this restriction and the lower end of which ($\sim$0–5 km) is not. It would be challenging but possible to determine the $\delta^{18}O$ values of individual olivine crystals from known crystallization depths; we suggest such measurements are an attractive goal for testing and/or elaborating this hypotheses.

[57] Perhaps the greatest strength of the model illustrated in Figure 11b is that it explains the association of low-$\delta^{18}O$ values with relatively low $^{3}He/^{4}He$ and low $^{208}Pb^{*}/^{206}Pb^{*}$ at moderate $^{206}Pb/^{204}Pb$ (Figures 7 and 8), and is consistent with evidence suggesting the low-$\delta^{18}O$ component is relatively low in $^{87}Sr/^{86}Sr$ and high in ε_{Hf} (Figure 6). All of these isotopic shifts are consistent with addition to primary Hawaiian magmas of a component derived from the local asthenosphere and/or lithosphere [*Huang and Frey*, 2003; Kurz, submitted manuscript, 2003; *Eisele et al.*, 2003].

[58] Major-element and rare earth-element data for these samples, as well as previous Os isotope data for samples from the HSDP-I core, place restrictions on this model. The lowest $\delta^{18}O$ values in Mauna Kea lavas are associated with low Al_2O_3/TiO_2 and high Sm/Yb ratios, consistent with them sampling a component resembling post shield and post-erosional lavas (Figures 7 and 8). These characteristics can be explained by low degrees of melting of an ultramafic source [*Chen and Frey*,

1983; *Feigenson et al.*, 2003; *Hirose and Kushiro*, 1993; *Baker et al.*, 1995]. Furthermore, previous work shows that low-$\delta^{18}O$ Hawaiian lavas have Os isotope compositions like those of most other terrestrial basalts rather than relatively radiogenic compositions expected of old basaltic rocks. This also suggests the low-$\delta^{18}O$ component is ultramafic (or very young, as in the model discussed in the previous section). Therefore, in the context of the model depicted in Figure 11b, the low-$\delta^{18}O$ component must come from olivine-rich rocks in the Pacific plate, where intrusion and gradual heating produces low degree melts that mix with infiltrating plume-derived magma. In the context of this model, the stratigraphic trend in geochemistry of the upper ~1/3 of the Mauna Kea section reflects greater proportions of lithospheric melt in deep magmatic plumbing systems as the volcano moves off the plume axis and the flux of plume-derived magma decreases.

[59] The principle weakness of the model discussed in this section is that it provides no obvious explanation for the relatively sharp decrease in $\delta^{18}O$ of coarse olivine phenocrysts going from the submarine to subaerial Mauna Kea sections, nor the similarity between oxygen-isotope stratigraphy and the modality of fractionation-normalized SiO_2 (Figure 5).

[60] Both of the models examined above provide explanations of some observations but not others. Therefore we conclude that low-$\delta^{18}O$ values of Hawaiian magmas reflect contamination rather than a low-$\delta^{18}O$ plume component, but that the origin of those contaminants and the places and mechanisms by which they were incorporated remain an open question. Future studies that could help discriminate between these models include (1) comparisons of the oxygen isotope geochemistry of rift zones on Mauna Loa and Kilauea (which should vary systematically with geography if the model illustrated in Figure 11a is correct) and (2) studies of the relationship between crystallization pressure, Mg# and $\delta^{18}O$ in individual olivine phenocrysts, which could establish whether low-$\delta^{18}O$ phenocrysts form at the high-pressures required of the model in Figure 11b, or only at the low pressures indicated by the model in Figure 11a.

[61] Finally, we emphasize that the preceding conclusions are based on the geochemical properties of low-$\delta^{18}O$ Mauna Kea lavas and should not be generalized to apply to the processes responsible for anomalously *high* $\delta^{18}O$ values previously found in Koolau and Lanai lavas [*Eiler et al.*, 1996b]. These values were initially interpreted to reflect the presence of a high-$\delta^{18}O$, recycled crustal component in the Hawaiian plume—a conclusion supported by subsequent radiogenic isotope studies [*Lassiter and Hauri*, 1998; *Blichert-Toft et al.*, 1999]. Furthermore, *Ducea et al.* [2002] subsequently discovered anomalously high-$\delta^{18}O$ mantle xenoliths from Oahu having radiogenic isotope compositions indicating they were infiltrated and metasomatized by plume-derived melt. Thus the high-$\delta^{18}O$, "Koolau-like" signature must have been carried by plume-derived melts before they ascended through the lithosphere.

Acknowledgments

[62] We thank all participants in the Hawaiian Scientific Drilling Project for their work in recovering, documenting and preparing the HSDP II core. We particularly thank authors of accompanying articles in this theme for providing us their data prior to its publication and Caroline Seamen for helping disseminate those data. We thank Paul Asimow for his help in performing calculations using the MELTS program, and H.P. Taylor, George Rossman, Edwin Schauble, Liz Johnson, Ronit Kessel and Sujoy Mukhopadhyay for helpful discussions of this and related work. We thank Mike Garcia, Don DePaolo and an anonymous reviewer for helpful comments on the initial draft of this manuscript. This research was partially supported by National Science Foundation grants OCE-0095897 and OCE-0112132.

References

Albarede, F., How deep do common basaltic magmas form and differentiate?, *J. Geophys. Res.*, *97*, 10,997–11,009, 1992.

Aldanmaz, E., J. A. Pearce, M. F. Thirlwall, and J. G. Mitchell, Petrogenetic evolution of late Cenozoic, post-collision volcanism in western Anatolia, Turkey, *J. Volcanol. Geothermal Res.*, *102*, 67–95, 2000.

Anderson, A. T., and G. G. Brown, CO_2 contents and formation pressures of some Kilauean melt inclusions, *Am. Mineral.*, *78*, 794–803, 1993.

Anderson, A. T., R. N. Clayton, and T. K. Mayeda, Oxygen isotope thermometry of mafic igneous rocks, *J. Geol.*, *79*, 714–729, 1971.

Appora, I., J. M. Eiler, A. Matthews, and E. M. Stolper, Experimental determination of oxygen isotope fractionations

between CO_2 and soda-melilite melt, *Geochim. Cosmochim. Acta*, *67*, 459 –471, 2002.

Baker, M. B., M. M. Hirschmann, M. S. Ghiorso, and E. M. Stolper, Compositions of near-solidus peridotite melts from experiments and thermodynamic calculations, *Nature*, *375*, 308–311, 1995.

Baker, M. B., S. Alves, and E. M. Stolper, Petrography and petrology of the Hawaii Scientific Drilling Project lavas: Inferences from olivine phenocrysts abundances and compositions, *J. Geophys. Res.*, *101*, 11,715–11,727, 1996.

Bergantz, G. W., Underplating and partial melting—Implications for melt generation and extraction, *Science*, *245*, 1093–1095, 1989.

Bindeman, I. N., and J. W. Valley, Low-delta O-18 rhyolites from Yellowstone: Magmatic evolution based on analyses of zircons and individual phenocrysts, *J. Petrol.*, *42*, 1491–1517, 2001.

Blichert-Toft, J., F. A. Frey, and F. Albarede, Hf isotope evidence for pelagic sediments in the source of Hawaiian basalts, *Science*, *285*, 879–882, 1999.

Blichert-Toft, J., D. Weis, C. Maerschalk, A. Agranier, and F. Albarède, Hawaiian hot spot dynamics as inferred from the Hf and Pb isotope evolution of Mauna Kea volcano, *Geochem. Geophys. Geosyst.*, *4*(2), 8704, doi:10.1029/2002GC000340, 2003.

Chauvel, C., and J. Blichert-Toft, A hafnium isotope and trace element perspective on melting of the depleted mantle, *Earth Planet. Sci. Lett.*, *190*, 137–151, 2001.

Chen, C. Y., and F. A. Frey, Origin of Hawaiian tholeiite and alkalic basalt, *Nature*, *302*, 785–789, 1983.

Clague, D. A., J. G. Moore, J. E. Dixon, and W. B. Friesen, Petrology of submarine lavas from Kilaueas Puna ridge, Hawaii, *J. Petrol.*, *36*, 299–349, 1995.

Ducea, M., G. Sen, J. M. Eiler, and J. Fimbres, Melt depletion and subsequent metasomatism in the shallow mantle beneath Koolau volcano, Oahu (Hawaii), *Geochem. Geophys. Geosyst.*, *3*(2), 1015, doi:10.1029/2001GC000184, 2002.

Eiler, J. M., Oxygen isotope variations of basaltic lavas and upper mantle rocks, in *Stable Isotope Geochemistry*, edited by J. W. Valley and D. R. Cole, *Rev. Mineral.*, *43*, 319–364, 2001.

Eiler, J. M., J. W. Valley, C. M. Graham, and L. P. Baumgartner, Ion microprobe evidence for the mechanisms of stable isotope retrogression in high-grade metamorphic rocks, *Contrib. Mineral. Petrol.*, *118*, 365–378, 1995.

Eiler, J. M., J. W. Valley, and E. M. Stolper, Oxygen isotope ratios in olivine from Hawaii Scientific Drilling Project, *J. Geophys. Res.*, *101*, 11,807–11,813, 1996a.

Eiler, J. M., K. A. Farley, J. W. Valley, A. W. Hofmann, and E. M. Stolper, Oxygen isotope constraints on the sources of Hawaiian volcanism, *Earth Planet. Sci. Lett.*, *144*, 453–468, 1996b.

Eiler, J. M., K. A. Farley, J. W. Valley, E. Hauri, H. Craig, S. R. Hart, and E. M. Stolper, Oxygen isotope variations in ocean island basalt phenocrysts, *Geochim. Cosmochim. Acta*, *61*, 2281–2293, 1997.

Eiler, J. M., A. Crawford, T. Elliott, K. A. Farley, J. W. Valley, and E. M. Stolper, Oxygen isotope geochemistry of oceanic-arc lavas, *J. Petrol.*, *41*, 229–256, 2000a.

Eiler, J. M., P. Schiano, N. Kitchen, and E. M. Stolper, Oxygen isotope evidence for recycled crust in the sources of mid-ocean ridge basalts, *Nature*, *403*, 530–534, 2000b.

Eiler, J. M., K. Gronvold, and N. Kitchen, Oxygen isotope evidence for the origin of geochemical variations in lavas from Theistareykir volcano in Iceland's northern neovolcanic zone, *Earth Planet. Sci. Lett.*, *184*, 269–286, 2000c.

Eisele, J., W. Abouchami, S. J. G. Galer, and A. W. Hofmann, The 320 kyr Pb isotope evolution of Mauna Kea lavas recorded in the HSDP-2 drill core, *Geochem. Geophys. Geosyst.*, *4*(5), 8710, doi:10.1029/2002GC000339, 2003.

Feigenson, M. D., L. L. Bolge, M. J. Carr, and C. T. Herzberg, REE inverse modeling of HSDP2 basalts: Evidence for multiple sources in the Hawaiian plume, *Geochem. Geophys. Geosyst.*, *4*(2), 8706, doi:10.1029/2001GC000271, 2003.

Galer, S. J. G., and R. K. O'Nions, Residence time of thorium, uranium and lead in the mantle with implications for mantle convection, *Nature*, *316*, 778–782, 1985.

Garcia, M. O., D. W. Muenow, K. E. Aggrey, and J. R. O'Neil, Major element, volatile and stable isotope geochemistry of Hawaiian submarine tholeiitic glasses, *J. Geophys. Res.*, *94*, 10,525–10,538, 1989.

Garcia, M. O., B. A. Jorgenson, J. J. Mahoney, E. Ito, and A. J. Irving, An evaluation of temporal geochemical evolution of Loihi summit lavas: Results from Alvin submersible dives, *J. Geophys. Res.*, *98*, 537–550, 1993.

Garcia, M. O., E. Ito, J. M. Eiler, and A. J. Pietraszka, Crustal contamination of Kilauea volcano magmas revealed by oxygen isotope analyses of glass and olivine from Puu Oo eruption lavas, *J. Petrol.*, *39*, 803–817, 1998.

Garlick, G. D., I. D. MacGregor, and D. E. Vogel, Oxygen isotope ratios in eclogites from kimberlites, *Science*, *172*, 1025–1027, 1971.

Gazis, C., H. P. Taylor Jr., K. Hon, and A. Tsvetkov, Oxygen isotopic and geochemical evidence for a short-lived, high-temperature hydrothermal event in the Chegem caldera, Caucasus mountains, Russia, *J. Volcanol. Geotherm. Res.*, *73*, 213–244, 1996.

Ghiorso, M. S., M. M. Hirchmann, and R. O. Sack, New software models thermodynamics of magmatic systems *Eos Trans. AGU*, *75*, 571–576, 1994.

Green, T. H., Experimental studies of trace-element partitioning applicable to igneous petrogenesis—Sedona 16 years later, *Chem. Geol.*, *117*, 1–36, 1994.

Gregory, R. T., and H. P. Taylor Jr., An oxygen isotope profile in a section of cretaceous oceanic crust, Samail ophiolite, Oman: Evidence for $\delta^{18}O$ buffering of the oceans by deep (>5 km) seawater-hydrothermal circulation at mid-ocean ridges, *J. Geophys. Res.*, *86*, 2737–2755, 1981.

Harmon, R. S., and J. Hoefs, Oxygen isotope heterogeneity of the mantle deduced from global ^{18}O systematics of basalts from different geotectonic settings, *Contrib. Mineral. Petrol.*, *120*, 95–114, 1995.

Hauri, E. H., Major-element variability in the Hawaiian plume, *Nature*, *382*, 415–419, 1996.

Hegner, E., D. M. Unruh, and M. Tatsumoto, Nd-Sr-Pb isotope constraints on the sources of West Maui volcano, Hawaii, *Nature*, *319*, 478–480, 1986.

Hildreth, W., and S. Moorbath, Crustal contributions to arc magmatism in the Andes of central Chile, *Contrib. Mineral. Petrol.*, *98*, 455–489, 1988.

Hirose, K., and I. Kushiro, Partial melting of dry peridotites at high pressures: Determination of compositions of melts segregated from peridotite using aggregates of diamond, *Earth. Planet. Sci. Lett.*, *114*, 477–489, 1993.

Hofmann, A. W., and K. P. Jochum, Source characteristics derived from very incompatible trace elements in Mauna Loa and Mauna Kea basalts, Hawaii Scientific Drilling Project, *J. Geophys. Res.*, *101*, 11,831–11,839, 1996.

Holt, E. W., and H. P. Taylor Jr., O-18/O-16 mapping and hydrogeology of a short-lived (approximate to 10 years) fumarolic (>500 degrees C) meteoric-hydrothermal event in the upper part of the 0.76 Ma Bishop Tuff outflow sheet, California, *J. Volcanol. Geothermal Res.*, *83*, 115–139, 1998.

Huang, S. C., and F. A. Frey, Trace element abundances of Mauna Kea basalt from Phase 2 of the Hawaii Scientific Drilling Project: Petrogenetic implications of correlations with major element content and isotopic ratios, *Geochem. Geophys. Geosyst.*, *4*(6), 8711, doi:10.1029/2002GC000322, 2003.

Kempton, P. D., J. G. Fitton, A. D. Saunders, G. M. Nowell, R. N. Taylor, B. S. Hardarson, and G. Pearson, The Iceland plume in space and time: A Sr-Nd-Pb-Hf study of the north Atlantic rifted margin, *Earth Planet. Sci. Lett.*, *177*, 255–271, 2000.

Kennedy, A. K., S.-T. Kwon, F. A. Frey, and H. B. West, The isotopic composition of postshield lavas from Mauna Kea volcano, Hawaii, *Earth Planet. Sci. Lett.*, *103*, 339–353, 1991.

Kyser, T. K., J. R. O'Neil, and I. S. E. Carmichael, Oxygen isotope thermometry of basic lavas and mantle nodules, *Contrib. Mineral. Petrol.*, *77*, 11–23, 1981.

Kyser, T. K., J. R. O'Neil, and I. S. E. Carmichael, Genetic relations among basic lavas and Ultramafic nodules: Evidence from oxygen isotope compositions, *Contrib. Mineral. Petrol.*, *81*, 88–102, 1982.

Lassiter, J. C., and E. H. Hauri, Osmium-isotope variations in Hawaiian lavas; evidence for recycled oceanic lithosphere in the Hawaiian Plume, *Earth Planet. Sci. Lett.*, *164*, 483–496, 1998.

Lassiter, J. C., D. J. DePaolo, and M. Tatsumoto, Isotopic evolution of Mauna Kea volcano: Results from the initial phase of the Hawaii Scientific Drilling Project, *J. Geophys. Res.*, *101*, 11,769–11,780, 1996.

Lassiter, J. C., E. H. Hauri, P. W. Reiners, and M. O. Garcia, Generation of Hawaiian post-erosional lavas by melting of a mixed lherzolite/pyroxenite source, *Earth Planet. Sci. Lett.*, *178*, 269–284, 2000.

Matthews, A., E. M. Stolper, J. M. Eiler, and S. Epstein, Oxygen isotope fractionation among melts, minerals, and rocks, *Min. Mag.*, *62A*, 971–972, 1998.

Miller, J. A., I. Cartwright, I. S. Buick, and A. C. Barnicoat, An O-isotope profile through the HP-LT Corsican ophiolite, France and its implications for fluid flow during subduction, *Chem. Geol.*, *178*, 43–69, 2001.

Moore, J. G., Density of basalt core from Hilo drill hole, Hawaii, *J. Volcanol. Geothermal Res.*, *112*, 221–230, 2001.

Muehlenbachs, K., Alteration of the oceanic crust and the ^{18}O history of seawater, in *Stable Isotopes in High Temperature Geological Processes*, edited by J. W. Valley, H. P. Taylor Jr., and J. R. O'Neil, *Rev. Mineral.*, *16*, 425–444, 1986.

Muehlenbachs, K., and G. Byerly, ^{18}O enrichment of silicic magmas caused by crystal fractionation at the Galapagos spreading center, *Contrib. Mineral. Petrol.*, *79*, 76–79, 1982.

Muehlenbachs, K., and I. Kushiro, Oxygen isotope exchange and equilibrium of silicates with CO_2 or O_2, *Year Book Carnegie Inst. Washington*, *71*, 232–236, 1974.

Reoder, E., Liquid CO_2 inclusions in olivine-bearing nodules and phenocrysts from basalts, *Am. Mineral.*, *50*, 1746–1782, 1965.

Ryerson, F. J., W. B. Durham, D. J. Cherniak, and W. A. Lanford, Oxygen diffusion in olivine: Effect of oxygen fugacity and implications for creep, *J. Geophys. Res.*, *94*, 4105–4118, 1989.

Schiano, P., J. Birck, and C. J. Allegre, Osmium-strontium-neodymium-lead isotopic covariations in mid-ocean-ridge basalt glasses and the heterogeneity of the upper mantle, *Earth Planet. Sci. Lett.*, *150*, 363–379, 1997.

Shanks, W. C., III, Stable isotopes in seafloor hydrothermal systems, in *Stable Isotope Geochemistry*, edited by J. W. Valley and D. R. Cole, *Rev. Mineral.*, *43*, 469–526, 2001.

Sharp, Z. D., A laser based microanalytical method for the in situ determination of oxygen isotope ratios of silicates and oxides, *Geochim. Cosmochim. Acta*, *54*, 1353–1357, 1990.

Valley, J. W., and C. M. Graham, Cryptic grain-scale heterogeneity of oxygen isotope ratios in metamorphic magnetite, *Science*, *259*, 1729–1733, 1993.

Valley, J. W., N. Kitchen, M. J. Kohn, C. R. Niendorf, and M. J. Spicuzza, UWG-2, a garnet standard for oxygen isotope ratio: Strategies for high precision and accuracy with laser heating, *Geochim. Cosmochim, Acta*, *59*, 5223–5231, 1995.

Walther, J. V., and P. M. Orville, Volatile production and transport in regional metamorphism, *Contrib. Mineral. Petrol.*, *79*, 252–257, 1982.

West, H. B., and W. P. Leeman, Isotopic evolution of lavas from Haleakala crater, Hawaii, *Earth Planet. Sci. Lett.*, *84*, 211–225, 1987.

White, W. M., A. W. Hofmann, and H. Puchelt, Isotope geochemistry of Pacific mid-ocean ridge basalt, *J. Geophys. Res.*, *92*, 4881–4893, 1987.